Published in final edited form as:
Nature. 2015 December 17; 528(7582): 409–412. doi:10.1038/nature15764.

Repairing oxidized proteins in the bacterial envelope using respiratory chain electrons

Alexandra Gennaris[#1,2,3], **Benjamin Ezraty**[#4], **Camille Henry**[4], **Rym Agrebi**[1,2,3], **Alexandra Vergnes**[4], **Emmanuel Oheix**[5], **Julia Bos**[4,†], **Pauline Leverrier**[1,2,3], **Leon Espinosa**[4], **Joanna Szewczyk**[1,2,3], **Didier Vertommen**[2], **Olga Iranzo**[5], **Jean-François Collet**[1,2,3,**], and **Frédéric Barras**[4,**]

[1]WELBIO, Avenue Hippocrate 75, 1200 Brussels, Belgium.

[2]de Duve Institute, Université catholique de Louvain, Avenue Hippocrate 75, 1200 Brussels, Belgium.

[3]Brussels Center for Redox Biology, Avenue Hippocrate 75, 1200 Brussels, Belgium.

[4]Aix-Marseille Université, CNRS, Laboratoire de Chimie Bactérienne, UMR 7283, Institut de Microbiologie de la Méditerranée, 31 Chemin Joseph Aiguier, 13009 Marseille, France.

[5]Aix-Marseille Université, Centrale Marseille, CNRS, iSm2 UMR 7313, 13397, Marseille, France

[#] These authors contributed equally to this work.

Abstract

The reactive species of oxygen (ROS) and chlorine (RCS) damage cellular components, potentially leading to cell death. In proteins, the sulfur-containing amino acid methionine (Met) is converted to methionine sulfoxide (Met-O), which can cause a loss of biological activity. To rescue proteins with Met-O residues, living cells express methionine sulfoxide reductases (Msrs) in most subcellular compartments, including the cytosol, mitochondria and chloroplasts [1-3]. Here, we report the identification of an enzymatic system, MsrPQ, repairing Met-O containing proteins in the bacterial cell envelope, a compartment particularly exposed to the ROS and RCS generated by the host defense mechanisms. MsrP, a molybdo-enzyme, and MsrQ, a heme-binding membrane protein, are widely conserved throughout Gram-negative bacteria, including major human pathogens. MsrPQ synthesis is induced by hypochlorous acid (HOCl), a powerful antimicrobial released by neutrophils. Consistently, MsrPQ is essential for the maintenance of envelope integrity under bleach stress, rescuing a wide series of structurally unrelated periplasmic proteins from Met

[**]Correspondence and requests for materials should be addressed to F.B. (barras@imm.cnrs.fr) or J.-F.C. (jfcollet@uclouvain.be) .
[†]Present address: Department of Physics, Princeton University, Princeton NJ-08544 USA.

AUTHOR CONTRIBUTIONS

F.B., J.-F.C., A.G. and B.E. wrote the paper. A.G., B.E., C.H., A.V., L.E., J.-F.C. and F.B. designed and performed the experiments. A.G., B.E., C.H., J.B., P.L. and J.S. constructed the strains and cloned the constructs. F.B., J.-F.C., A.G., B.E., and C.H. analyzed and interpreted the data. D.V. performed MS analyses. E.O. and O.I. prepared the diastereoisomers. R.A. performed bioinformatic analyses. All authors discussed the results and commented on the manuscript.

SUPPLEMENTARY INFORMATION is linked to the online version of the paper at www.nature.com/nature

The authors declare no competing financial interests.

Europe PMC Funders Author Manuscripts

oxidation, including the primary periplasmic chaperone SurA. For this activity, MsrPQ uses electrons from the respiratory chain, which represents a novel mechanism to import reducing equivalents into the bacterial cell envelope. A remarkable feature of MsrPQ is its capacity to reduce both *R*- and *S*- diastereoisomers of Met-O, making this oxidoreductase complex functionally different from previously identified Msrs. The discovery that a large class of bacteria contain a single, non-stereospecific enzymatic complex fully protecting Met residues from oxidation should prompt search for similar systems in eukaryotic subcellular oxidizing compartments, including the endoplasmic reticulum (ER).

The fact that no Msr had been identified in the cell envelope of important human pathogens, including *Escherichia coli* and *Pseudomonas aeruginosa*, was surprising as this compartment is particularly exposed to the oxidizing compounds present in the environment. We postulated that such a Met-O reducing system had remained unidentified, and applied a genetic approach to uncover it, using *E. coli* as a model. We first constructed an *E. coli* Met auxotroph mutant lacking all cytoplasmic Msrs and found this strain (JB590) to be unable to use Met-O as the only Met source (Fig. 1a). We then searched for suppressor mutations conferring Met-O reducing capacity to JB590, which led to the isolation of strain BE100 (Fig. 1a). Genetic analysis of the suppressor revealed the presence of an insertion sequence element (IS2) within *yedV*, a gene coding for the histidine kinase of the uncharacterized YedV/YedW two-component system [4]. In close vicinity were two genes, *yedY* and *yedZ*, encoding, respectively, a periplasmic molybdopterin-containing oxidoreductase and its putative membrane redox partner [5,6]. YedY had been shown to reduce a variety of substrates *in vitro*, including trimethylamine N-oxide, and dimethyl, methionine and tetramethylene sulfoxides [5]. However, its physiological function had remained elusive, although a recent study in *Azospira suillum* suggested the homologous protein to be important for HOCl resistance [7]. We found that insertion of the IS2 led to a 100-fold increase in the levels of the *yedYZ* mRNA in strain BE100 and to higher YedY protein levels (Fig. 1b). Deletion of either *yedY* or *yedZ* prevented BE100 to grow on Met-O (Fig. 1a, Extended Data Table 1), while the simultaneous overproduction of YedY and YedZ, but not of YedY or YedZ alone, rendered the parental strain JB590 able to use Met-O (Extended Data Table 1). Altogether, these results indicated that the ability of the suppressor strain BE100 to reduce Met-O resulted from the increased synthesis of YedY and YedZ, implying that these two proteins function together as an Msr system. Growth of the BE100 strain was dependent on *moeA,* a gene required for the synthesis of molybdopterin cofactors, and on *tatC*, encoding a protein required for the translocation of metalloenzymes across the inner membrane (IM) (Fig. 1a). Exposure of wild-type cells to HOCl, but not to H_2O_2, induced the synthesis of YedY to levels comparable to those observed in BE100 (Fig. 1c), indicating that these proteins are specifically expressed in response to bleach stress. Interestingly, induction by HOCl was dependent on the presence of a functional YedV/YedW system (Extended Data Fig. 1).

All previously identified Msrs rely on electrons derived from NADPH *via* the thioredoxin system for activity [1]. This was not the case for YedYZ, as deletion of *trxA*, encoding the thioredoxin responsible for Msr recycling [8], had no effect on the ability of BE100 to reduce Met-O (Fig. 1a). As YedZ contains a *b*-type heme [9], a cofactor typically associated with the quinone oxidizing cytochrome *b* of the respiratory chain complexes, we considered the

respiratory chain as a potential electron source. Deletion of *menA* and *ubiE*, two genes required for quinone synthesis, prevented BE100 from utilizing Met-O (Extended Data Table 1), supporting a model in which YedZ uses electrons derived from the IM pool of mature quinones to provide reducing equivalents to YedY (Extended Data Fig. 2). From now on, YedY and YedZ will be referred to as MsrP (for periplasm) and MsrQ (for quinone), respectively.

We then tested whether MsrPQ, in addition to free Met-O, also rescued Met-O residues present in proteins. Purified MsrP was shown to reduce N-acetyl-Met-O, a substrate mimicking protein-bound Met-O (Extended Data Fig. 3a), with a K_m of 3.8 ± 1.2 mM, in line with the values reported for other Msrs [10]. Note that in the experiments involving purified MsrP, electrons were provided to the oxidoreductase by an inorganic system reducing molybdoenzymes [11]. Next, we tested the ability of MsrP to reduce oxidized calmodulin (CaMox), a substrate commonly used to assess Msr activity. We used a gel shift assay based on the reduced mobility exhibited in SDS-PAGE by proteins containing Met-O [12]. Incubation of CaMox with MsrP restored its mobility, suggesting that MsrP was able to reduce Met-O residues in CaMox (Fig. 2a). This was confirmed by showing with LC-MS/MS that the oxidized Met residues that could be detected in CaMox were reduced back to levels similar to those observed in CaM following incubation with MsrP (Fig. 2b). Altogether, these results indicated that MsrP is able to reduce protein-bound Met-O.

Upon oxidation, two diastereoisomers of Met-O can form, referred to as *R* and *S,* owing to the asymmetric position of the oxidized sulfur atom in the lateral chain (Fig. 2c). All Msrs described so far exhibit stereospecificity, specifically reducing either the *R* (MsrB, MsrC) or the *S* isoform (MsrA, BisC). Using highly pure diastereoisomers (Extended Data Fig. 4), we found MsrP to exhibit activity towards both (Fig. 2d), with K_m values of 25.7 ± 4.7 mM and 8.0 ± 2.7 mM for *R*- and *S*-Met-O, respectively (Extended Data Fig. 3b). Accordingly, the BE100 suppressor strain was able to use *R* and *S* Met-O (Fig. 2e), in contrast to strains expressing single stereospecific Msrs (Extended Data Fig. 3c). Thus, MsrP is a new type of Msr with no stereospecificity.

To search for the physiological substrates of MsrP, periplasmic proteins from a Δ*msrP* mutant were oxidized with HOCl, incubated with MsrP and subjected to a semi-quantitative 2D-LC-MS/MS analysis. 20 proteins that had one or more HOCl-oxidized Met residues that MsrP could reduce were identified (Extended Data Table 2). Using gel shift assays in combination with LC-MS/MS analysis, we confirmed the ability of MsrP to reduce the chaperone SurA and the lipoprotein Pal (Fig. 3a-b). Altogether these results established that MsrP is able to repair a wide panel of structurally and functionally diverse periplasmic proteins *in vitro*.

SurA is the primary periplasmic chaperone, escorting most β-barrel proteins to the outer membrane (OM) [13,14]. As HOCl-oxidized SurA loses its chaperone activity (Fig. 4a), we used this property to probe the physiological importance of the MsrPQ system. First, we showed that SurA could be oxidized *in vivo* by HOCl and that expression of the MsrPQ system, but not of MsrP alone, restored its mobility (Fig. 3c). Similar results were obtained for Pal (Fig. 3d), confirming that MsrP and MsrQ collaborate in the protection of SurA and

Pal from oxidative damage. We then tested if the repair of SurA by MsrP, which restores the activity of the chaperone *in vitro* (Fig. 4a), was important to keep SurA active under HOCl stress. For this, we used a mutant strain lacking the chaperone Skp, in which SurA becomes essential [15,16]. We found that deleting *msrP* rendered the Δ*skp* strain hypersensitive to HOCl (Fig. 4b), suggesting that oxidized, inactive SurA accumulates in the absence of MsrP. In agreement with this, the sensitivity of the Δ*skp*Δ*msrP* mutant to HOCl was suppressed by overexpression of SurA (Fig. 4c). Further highlighting the need to protect Met residues in periplasmic proteins, HOCl-pretreated Δ*msrP* mutants were found to be more sensitive to SDS, a phenotype indicative of defects in the OM (Fig. 4d) [17].

The conservation of MsrPQ throughout Gram-negative bacteria (Extended Data Fig. 5-6) illustrates the importance of having a Met-O reducing system in the periplasm. *Neisseria* species stand out as an exception in lacking MsrPQ. However, in these bacteria, evolutionary tinkering generated an envelope hybrid protein combining two classic stereospecific Msr domains [18]. A remarkable feature of MsrPQ is that its rescue activity depends on electrons provided by the respiratory chain. This represents an entirely novel way to provide reducing power for protein quality control in the envelope. Indeed, known-reducing systems functioning in the periplasm use electrons provided by the IM protein DsbD and thioredoxin [19]. Hence, diverting electrons from the respiratory chain to control extracytosolic protein quality is an unprecedented link between metabolism and cellular integrity.

The chaperone SurA is one of the targets of the MsrPQ system. Having a protein folding helper under the control of a repair system reveals an additional layer in the complex periplasmic protein quality control network. Testing if this system is an attractive target for antimicrobial development, as suggested by the colonization defect exhibited by the *msrP* mutant in *Campylobacter jejuni* [20], will be fields of future research. By highlighting the importance of protecting proteins targeted to oxidizing compartments, our work calls for a detailed investigation of the process of Met-O reduction in the ER, where only an *R*-Met-O specific MsrB has been identified [3]. As long speculated, a possibility would be that the ER contains an epimerase catalyzing the interconversion of *R*- and *S*-Met-O. Alternatively, in light of the present study, the ER could contain a novel Met-O reducing system yet to be discovered.

METHODS

Strains and microbial techniques

The strains used in this study are listed in Supplementary Table 1. Unless otherwise specified, for all deletion mutants, the corresponding alleles from the Keio collection [22] were transferred into the MC4100 wild-type strain using P1 transduction standard procedures [23] and checked by PCR. To excise the resistance cassette, we used pCP20 [22,24]. Strain AG227, deleted for the entire *yedYZ* operon, was constructed as follows. First, a *cat-sacB* cassette, encoding chloramphenicol acetyl transferase and SacB, a protein conferring sensitivity to sucrose, was amplified from strain CH1990 using primers *yedYZ::cat-sacB*_Fw and *yedYZ::cat-sacB*_Rv. The resulting PCR product shared a 40-bp homology to the 5′ UTR of *yedY* (*msrP)* and to the 3′ UTR of *yedZ* (*msrQ)* at its 5′ and 3′ ends, respectively. After

purification, the PCR product was transformed by electroporation into CH1940. These cells harbor the pSIM5-tet vector, which encodes the Red recombination system proteins Gam, Beta and Exo under the control of the temperature-sensitive repressor cI859, encoded by the same vector. Induction of the Gam, Beta and Exo proteins was induced by shifting the cells to 42°C for 15 minutes prior to making them electrocompetent. Recombinant cells were selected on chloramphenicol-containing plates (25 μg/ml) at 37°C for 16h. At this temperature, the pSIM5-tet vector, which has a temperature-sensitive origin of replication, is lost. Colonies were also tested for the presence of the *cat-sacB* cassette by negative selection on sucrose-containing media (5% sucrose, no NaCl). Finally, we verified that the *cat-sacB* cassette replaced the *msrPQ* operon in the resulting strain (AG219) by sequencing across the junctions. The *cat-sacB* cassette was subsequently moved from AG219 to TP1004 by P1 transduction. The *cat-sacB* cassette was eliminated from the resulting strain (AG220) by transforming it with the pSIM5-tet plasmid, electroporating it with the oligonucleotide Delta_*yedYZ* (300 ng) and performing lambda red recombination as described above. Recombinants were selected on sucrose-containing media at 30°C for 16h. To eliminate the plasmid, the selected colonies were grown at 37°C for 16h. Loss of the cassette in the resulting AG227 strain was verified by positive (sucrose resistance) and negative (chloramphenicol sensitivity) selection and by PCR.

The *msrQ* deletion mutant (strain BE105) was generated using the PCR knockout method developed by Datsenko and Wanner [24]. Briefly, a DNA fragment containing the *cat* gene flanked with the homologous sequences found upstream and downstream of the *yedZ* gene was PCR-amplified using pKD3 as template and the oligonucleotides P1_Up_YedZ and P2_Down_YedZ. Strain BE100, carrying plasmid pKD46, was then transformed by electroporation with the amplified linear fragment. Chloramphenicol-resistant clones were selected and verified by PCR.

The *msrP::lacZ* fusion was constructed using the method described by Mandin and Gottesman [25]. Briefly, the *msrP* promoter region lying between nt −797 and nt +63, using the A nucleotide within the initiation triplet as a reference, was amplified by PCR with the appropriate oligonucleotides (*lacI-msrP*$_{\text{forward}}$ and *lacZ-msrP*′$_{\text{reverse}}$**)**. Using mini-lambda mediated recombineering, the PCR product was then directly recombined with the chromosome of a modified *E. coli* wild-type strain (PM1205), carrying a P_{BAD}-*cat-sacB* cassette inserted in front of *lacZ* ,at the 9th codon. Recombinants were selected for loss of the *cat-sacB* genes, resulting in the translational fusion of *msrP* to *lacZ.*

Plasmid construction

The plasmids and primers used in this study are listed in Supplementary Tables 2 and 3, respectively. The YedY-His_6 expression vector was constructed as follows. Site directed mutagenesis using primers pTAC_*NdeI*_Fw and pTAC_*NdeI*_Rv was performed using pTAC-MAT-Tag-2 as template in order to introduce an *Nde*I restriction site in the vector, yielding vector pAG177. *yedY* was amplified from the chromosome (MC4100) using primers pTAC_*yedY*_Fw and pTAC_*yedY*-His_6_Rv, which resulted in the fusion of a His_6 tag coding sequence at the 3′ end. The PCR product was subsequently cloned into pAG177 using *Nde*I and *Bgl*II restriction sites, generating plasmid pAG178. To construct IPTG-

inducible pTAC-MAT-Tag-2 vectors expressing either MsrP (without tag) or both MsrP and MsrQ, we first amplified the corresponding coding DNA sequences (*msrP* or the *msrPQ* operon) from the chromosome of strain MC4100 using primer pairs pTAC_*yedY*_Fw/ pTAC_*yedY*_Rv and pTAC_*yedY*_Fw/ pTAC_*yedZ*_Rv, respectively. The PCR products were then cloned into pAG177 using restriction sites *Nde*I and *Bgl*II, yielding pAG192 (MsrP) and pAG195 (MsrPQ). The complementation pAM238 vectors constitutively expressing either MsrP or MsrQ alone (without tag) or both MsrP and MsrQ were constructed as follows. We first amplified the corresponding coding DNA sequences (*msrP, msrQ,* or the *msrPQ* locus) in addition to a 50 bp upstream region from each start codon (in order to include a RBS) from the chromosome of strain MG1655 using primer pairs pAM238_*yedY*_Fw/ pAM238_*yedY*_Rv, pAM238_*yedZ*_Fw/ pAM238_*yedZ*_Rv and pAM238_*yedY*_Fw/ pAM238_*yedZ*_Rv, respectively. The PCR products were then cloned into pAM238 using restriction sites *KpnI* and *PstI*, yielding pAG264 (MsrP), pAG275 (MsrQ), and pAG265 (MsrPQ).

The vector allowing the arabinose-inducible expression of SurA was constructed as follows. The *surA*-encoding DNA and its 50 bp upstream region (in order to include a RBS) were amplified from the chromosome of strain MG1655 using the primer pair *surA*_Fw/*surA*_Rv. The PCR product was then cloned into pBAD33 using restriction sites *KpnI* and *XbaI,* yielding vector pAG290.

Analysis of the *yedYZ* operon expression by RT-qPCR

Expression levels of the *yedYZ (msrPQ)* mRNA were assessed in M63 minimal medium supplemented with 0.5% glycerol, 0.15% casaminoacids, 1 mM $MgSO_4$, 1 mM $MoNa_2O_4$, 17 μM $Fe_2(SO_4)_3$, and vitamins (thiamin 10 μg/ml, biotin 1 μg/ml, riboflavin 10 μg/ml, and nicotinamide 10 μg/ml). Overnight cultures of MG1655 were diluted to an A_{600} of 0.04 in fresh M63 minimal medium (100 ml) and cultured aerobically at 37°C until an A_{600} of 0.8. Cells (10 ml) were then pelleted, resuspended in TriPure (Roche) and homogenized. After mixing with chloroform, RNA was isolated by centrifugation (15 min, 15,700 × *g*, 4°C), precipitated with isopropanol, washed with ethanol 70%, dried and finally resuspended in DEPC water. Any residual DNA was eliminated by treatment of the sample with DNAse (Turbo DNA-free™ Kit, Ambion). The RevertAid RT kit (Thermo Scientific) was used to generate cDNA from 1 μg RNA extracted from each of the cultured strains. cDNAs were then diluted 1/10 and submitted to real time PCR (qPCR), using the qPCR Core kit for SYBR Green I No ROX (Eurogentec) and a MyiQ™ Single-Color Real-Time PCR Detection System (Bio-Rad). *yedYZ* expression levels were normalized to the expression of *gapA.* Primers used for qPCR analysis were: qPCR_*yedYZ*_Fw and qPCR_*yedYZ*_Rv for *yedYZ*, and qPCR_*gapA*_Fw and qPCR_*gapA*_Rv for *gapA* (Supplementary Table 3).

Immunoblot analysis of MsrP expression

Synthesis of MsrP in strains JB590 and BE100 was assessed as follows. Overnight cultures were diluted to an A_{600} of 0.04 in fresh M63 minimal medium (100 ml) and cultured aerobically at 37°C until an A_{600} value of 0.8. 900 μl of each culture were then precipitated with 10% ice-cold TCA, pellets were washed with ice-cold acetone, dried, resuspended and heated at 95°C in Laemmli SDS sample buffer (SB buffer) (2% SDS, 10% glycerol, 60 mM

Tris-HCl, pH 7.4, 0.01% bromophenol blue), and loaded on an SDS-PAGE gel for immunoblot analysis. The protein amounts loaded were standardized by taking into account the A_{600} values of the cultures.

To monitor the MsrP expression levels following NaOCl or H_2O_2 treatment, overnight cultures of wild-type cells (MG1655) were diluted to an A_{600} of 0.04 in fresh LB medium (100 ml) and grown aerobically at 37°C until to an A_{600} of 0.5. NaOCl (2 mM) or H_2O_2 (1 mM) was then added to the cultures. Samples were TCA-precipitated, washed with ice-cold acetone, dried, suspended in SB buffer, heated at 95°C, and loaded on an SDS-PAGE gel for immunoblot analysis. The protein amounts loaded were standardized by taking into account the A_{600} values of the cultures. The specificity of the anti-MsrP antibody was verified (Supplementary Figure 5).

Preparation of pure diastereoisomeric forms of Met-O

L-Methionine sulfoxide ($[\alpha]_D^{24}$ = +14.3 (water)), triethylamine (>99%), and methanol (>99.6%) were obtained from Sigma-Aldrich, picric acid from Prolabo, and D_2O from SDS. Water was purified using the Millipore Elix Essential 3 apparatus. ^1H and ^{13}C NMR were recorded on a Bruker Avance III Nanobay spectrometer (^1H: 400 MHz, $\{^1H\}^{13}C$: 100 MHz). Chemical shifts (δ) were referenced to dioxane (^1H: δ = 3.75 ppm; ^{13}C: δ = 67.19 ppm) [26], which was added as an internal reference, and resonances are detailed as follow, ^1H: δ in ppm (multiplicity, J-coupling in Hertz, integration, signal attribution); $\{^1H\}^{13}C$: δ in ppm (signal attribution). For each diastereoisomer, chemical shifts are similar to these previously reported [27]. ^{13}C resonance assignments were confirmed by HSQC experiments. Optical rotations were measured on an Anton Paar Modular Circular Polarimeter 200 instrument at 25°C and 589 nm from aqueous solution containing 0.8 – 1.2 g/100 ml of L-methionine sulfoxide. The values reported are the average and standard deviation relative to three independent measurements recorded on distinct solutions.

The commercial mixture of diastereoisomers was separated following the previously reported method [28]. Briefly, 10 ml of water was added to L-methionine sulfoxide (1.333 g, 8.069 mmol) and picric acid (1.849 g, 8.071 mmol). The suspension was heated to reflux until complete dissolution and then slowly cooled to room temperature. The suspension was filtered on sintered funnel and the solid was washed with cold water (10 ml in total). Both, the solid (*dextro*) and filtrate (*levo*) were collected separately for further purification.

dextro—To the dried solid, 20 ml of water were added and the mixture was heated to reflux and then allowed to cool down to room temperature slowly. The solid was filtered out, washed with 10 ml water, and dried. Again, 11 ml of methanol were added to the resulting solid and the mixture heated to reflux. Following slow cooling, the yellow crystals were filtered, washed with 5 ml methanol and dried. A portion was used for structure determination by X-ray analysis. To the dextrogyre picrate salt (1.345 g, 3.42 mmol), ~1.1 equivalents of triethylamine were added as a dilute aqueous solution (22 ml, 175 mM, 3.85 mmol). Subsequently, 200 ml of acetone were added portion-wise to the above stirring suspension and a white solid precipitated. This was filtered, washed, triturated with acetone and finally dried in vacuum (533 mg, 80%).

levo—The volume of the filtrate was reduced in vacuum at 40°C to about 3-4 ml in order to obtain a saturated solution and a little precipitate. Then, 1.5 ml of water were added, the suspension was filtered and the solid washed with minimal water (2 ml). The whole step was repeated once (reduce the volume, dilute, filter and wash), and the resulting solution was then completely dried in vacuum. To the resulting yellow residue, 15 ml of methanol were added and the suspension was heated to reflux. In our hands, no solid precipitated upon cooling down (in contrast with the reported method [28]), therefore the solution was dried again in vacuum. Following the same protocol as before, to the levogyre-enriched picrate salt (1.354 g, 3.44 mmol), ~1.1 equivalent of triethylamine were added as a concentrated aqueous solution (3.8 ml, 1 M, 3.8 mmol). Afterwards, 200 ml of acetone were added portion-wise and a white solid precipitated. This was filtered, washed, triturated with acetone and finally dried in vacuum (515 mg, 77%).

- *dextro* (L-methionine-*S*-sulfoxide): $[\alpha]_D^{25}$ = +99.2 ± 1.5 ° (water); ^{1}H NMR (400 MHz, D_2O pD = 6.5): 3.88 (t, ^{3}J = 6.3, 1 H, Hα_S), 3.02 (m, 2 H, Hγ_S), 2.74 (s, 3H, Hε_S), 2.31 (dd, J = 14.4, 7.6, 2H, Hβ_S); {^{1}H}^{13}C NMR (100 MHz, D_2O): 173.8 (COO$_S$), 54.0 (Cα_S), 48.9 (Cγ_S), 37.2 (Cε_S), 24.4 (Cβ_S).

  Literature values from[28]: $[\alpha]_D^{25}$ = +99 ° (water), from[27]: $[\alpha]_D$ = +98.2 ° (water, room temperature); ^{1}H NMR (300 MHz, D_2O): 4.10 (m, 1 H), 3.08-2.78 (m, 2 H), 2.59 (s, 3H), 2.32-2.13 (m, 2H); ^{13}C NMR (75 MHz, D_2O): 171.1, 52.0, 48.3, 37.0, 23.5.

- *levo* (L-methionine-*R*-sulfoxide): $[\alpha]_D^{25}$ = −72.7 ± 0.5 ° (water); ^{1}H NMR (400 MHz, D_2O pD = 6.5): 3.86 (t, ^{3}J = 6.3, 1 H, Hα_R), 3.12 (ddd, J = 13.4, 9.6, 7.0, 1 H, Hγ_{R1} or Hγ_{R2}), 3.02 (m, 2H, Hγ_S), 2.93 (ddd, J = 13.5, 9.1, 6.8, 1 H, Hγ_{R1} or Hγ_{R2}), 2.74 (s, 3H, Hε_R), 2.31 (m, 2H, Hβ_R); {^{1}H}^{13}C NMR (100 MHz, D_2O): 173.9 (COO$_R$), 54.2 (Cα_R), 54.0 (Cα_S), 48.9 (Cγ_R), 37.2 (Cε_S), 37.0 (Cε_R), 24.4 (Cβ_R).

  Literature values from [28]: $[\alpha]_D^{26}$ = −71.6 ° (water), from [27]: $[\alpha]_D$ = −78 ° (water, room temperature); ^{1}H NMR (300 MHz, D_2O): 4.10 (m, 1 H), 3.08-2.78 (m, 2 H), 2.59 (s, 3H), 2.32-2.13 (m, 2 H); ^{13}C NMR (75 MHz, D_2O): 171.1, 52.1, 48.4, 37.0, 23.7.

In the ^{1}H NMR spectra, the resonance centered at 3.02 ppm was attributed to the *S*-enantiomer. The relative integral values suggest that *R*-Met-O is contaminated by 3% of the *S*- diastereoisomer. Moreover, comparing the measured $[\alpha]_D^{25}$ values with those reported in [27], the data are consistent with the presence of 3% *S*- diastereoisomer as a contaminant. Such purity is in line with previous reports using the same separation method [28,29]. The absolute configuration of the L-methionine-*S*-sulfoxide was confirmed by X-Ray structural analysis and matches with previous assignments [27,30].

Synthesis of N-acetyl-Met-O

To synthesize N-acetyl-Met-O, Met-O (30 mg; Sigma-Aldrich) was solubilized in 2 ml 100% acetic acid. After addition of 2 ml of 97% acetic anhydride, the resulting mixture was incubated 2 h at 23°C. Then, 2 ml of water were added and the mixture was lyophilized overnight. Finally, the lyophilized N-acetyl-Met-O was washed 3 times with 6 ml of water,

re-lyophilized and suspended in 500 mM Na_2HPO_4, pH 9.0 to a final concentration of 1.5 M. The pH was then adjusted to 7 with NaOH.

Kinetic analysis of MsrP activity

The MsrP reductase activity was followed spectrophotometrically at 600 nm by monitoring the substrate-dependent oxidation of reduced benzyl viologen ($BVH^{\cdot+}$), serving as an electron donor. Reactions were carried out anaerobically at 30°C in degassed and nitrogen-flushed 50 mM MOPS, pH 7.0 using stoppered cuvettes. Benzyl viologen was used at a final concentration of 0.4 mM (ϵ of $BVH^{\cdot+}$ = 7,800 M^{-1} cm^{-1}) and reduced with sodium dithionite. The final reaction volume was kept constant, with the ordered addition of benzyl viologen, sodium dithionite, 1-32 mM N-acetyl-methionine sulfoxide (NacMet-O) and 10 nM MsrP-His_6. The concentrations used for the *R*- and *S*-Met-O diastereoisomers were 1-64 mM. The Michaelis-Menten parameters (V_{max} and K_m) were determined using the Graphpad Prism software.

Analysis of MsrA and MsrB activities

The reductase activities of MsrA and MsrB were followed spectrophotometrically at 340 nm by monitoring the substrate-dependent oxidation of NADPH (ϵ = 6,220 M^{-1} cm^{-1}). Reactions were carried out at 37°C in HEPES-KOH 20 mM, pH 7.4, NaCl 10 mM, and the final reaction volumes were kept constant, with the ordered addition of 250 μM NADPH (Roche), 2.6 μM of TrxR, 40 μM of Trx, 64 mM substrate and 1.5 μM of either MsrA or MsrB.

Identification of the periplasmic proteins repaired by MsrP using 2D-LC-MS/MS

The identification of the MsrP substrates was performed as follows. AG89 cells (2L) were grown aerobically at 37°C in terrific broth to an A_{600} of 0.8. Periplasmic extracts were prepared as described previously [31]. Briefly, cells were pelleted by centrifugation at 3,000 × *g* for 20 minutes at 4°C and incubated on ice with gentle shaking for 30 minutes in 100 mM Tris-HCl, pH 8.0, 20% sucrose, 1 mM EDTA. This mixture also contained 20 mM N-ethylmaleimide (NEM) in order to alkylate reduced cysteine residues in proteins to prevent their subsequent oxidation. Periplasmic proteins were then isolated by centrifugation of the cells at 3,000 × *g* for 20 minutes at 4°C. The periplasmic extract was subsequently concentrated by ultrafiltration in an Amicon cell (3,000 Da cutoff, YM-3 membrane) and loaded on a PD-10 column (GE healthcare) equilibrated with 50 mM NaPi, pH 8.0, 50 mM NaCl. After concentration using a 5 kDa cutoff Vivaspin 4 (Sartorius) concentrator, the extract was finally separated in 3 samples. Two samples were incubated 10 min at 37°C with 2 mM NaOCl while the third one was left untreated to serve as reduced control. NaOCl was then removed by gel filtration using a NAP-5 column (GE healthcare) equilibrated with 50 mM MOPS, pH 7.0. The untreated sample was also subjected to the NAP-5 gel filtration.

One of the NaOCl-oxidized fractions was then reduced *in vitro* by incubation for 1 h at 37°C with 10 μM MsrP, 10 mM benzyl viologen and an excess of sodium dithionite. The other NaOCl-oxidized fraction, used as an oxidized control, and the non-oxidized fraction were incubated with 10 mM benzyl viologen and an excess of sodium dithionite but without MsrP. The three samples were then desalted by dialysis against 50 mM MOPS, pH 7.0 by

Europe PMC Funders Author Manuscripts

using Slide-A-Lyzer 3,500 MWCO G2 cassettes (Thermo Scientific). The 3 samples (500 μg) were precipitated by adding TCA to a final concentration of 10% w/v. The resulting pellets were washed with ice-cold acetone, dried in a Speedvac, suspended in 0.1 M NH_4HCO_3, pH 8.0, and digested overnight at 30°C with 3 μg sequencing grade trypsin. 2D-LC-MS/MS analysis was performed essentially as described [32]. Briefly peptides were first separated on a first dimension Hydrophilic Interaction Chromatography (HILIC) column with a reverse ACN gradient and 25 fractions of 1 ml collected (2 min/fraction). After drying, peptides were analyzed by LC-MC/MS on a C18 column. The MS scan routine was set to analyze by MS/MS the five most intense ions of each full MS scan, dynamic exclusion was enabled to assure detection of co-eluting peptides.

Protein identification by mass spectrometry

Raw data collection of approximately 230,000 MS/MS spectra per 2D-LC-MS/MS experiment was followed by protein identification using SEQUEST. All MS raw files have been deposited to the ProteomeXchange Consortium [33] via the PRIDE partner repository with the dataset identifier PXD002804. In details, peak lists were generated using extract-msn (ThermoScientific) within Proteome Discoverer 1.4.1. From raw files, MS/MS spectra were exported with the following settings: peptide mass range: 350–5,000 Da, minimal total ion intensity 500. The resulting peak lists were searched using SequestHT against a target-decoy *E. coli* protein database (release 07.01.2008, 8,678 entries comprising forward and reversed sequences) obtained from Uniprot. The following parameters were used: trypsin was selected with proteolytic cleavage only after arginine and lysine, number of internal cleavage sites was set to 1, mass tolerance for precursors and fragment ions was 1.0 Da, considered dynamic modifications were + 15.99 Da for oxidized methionine, + 125.12 Da for NEM on cysteines. Peptide matches were filtered using the q-value and Posterior Error Probability calculated by the Percolator algorithm ensuring an estimated false positive rate below 5%. The filtered SEQUEST HT output files for each peptide were grouped according to the protein from which they were derived using the multiconsensus results tool within Proteome Discoverer. Then the peptides spectral matches values of only Met containing peptides were combined from the three 2D-LC-MS/MS and exported in a Microsoft Excel spreadsheet with the rows referring to the peptides sequences and the columns to the fractions of the HILIC column. Oxidation of Met residues to Met-O by NaOCl causes a hydrophilic shift, which influences their retention time and makes them elute later (4-8 min) than their reduced counterpart on a HILIC column. If these Met-O are reduced by MsrP, they will then show an hydrophobic shift and elute at the same retention time on the HILIC column than in the control sample. By comparing the retention times and the number of peptide spectral matches of the Met-O containing peptides in a periplasmic extract under three experimental conditions (control, oxidized by NaOCl with and without MsrP), one can identify “bona fide” potential MsrP substrates.

Protein expression and purification

TP1004 cells harboring plasmid pAG178 and over-expressing MsrP-His_6 protein, were grown aerobically at 30°C in terrific broth (Sigma-Aldrich) supplemented with sodium molybdate (1.5 mM) and ampicillin (200 μg/ml). When cells reached an A_{600} of 0.8, expression was induced with 0.1 mM IPTG for 3 h. Periplasmic proteins were then extracted

as in [32]. MsrP-His_6 was then purified by loading the periplasmic extract on a 1 ml HisTrap FF column (GE healthcare) equilibrated with buffer A (NaPi 50 mM, pH 8.0, NaCl 300 mM). After washing the column with buffer A, MsrP-His_6 was eluted by applying a linear gradient of imidazole (from 0 to 300 mM) in buffer A. The fractions containing MsrP-His_6 were pooled, concentrated using a 5 kDa cutoff Vivaspin 15 (Sartorius) device and desalted on a PD-10 column (GE Healthcare) equilibrated with 50 mM NaPi, pH 8.0, 150 mM NaCl.

VU1 calmodulin, MsrA and MsrB were expressed and purified as described previously [34,35].

Thioredoxin (Trx) was expressed and purified as follows. BL21 (DE3) cells harboring plasmid pMD205, over-expressing Trx with a C-terminal His_6 tag, were grown aerobically at 37°C in LB supplemented with kanamycin (50 μg/ml). Expression was induced at an A_{600} of 0.6 with 1 mM IPTG during 3 h. Cells were then pelleted, resuspended in buffer A (NaPi 50 mM, pH 8.0, NaCl 300 mM) and disrupted by 2 passes through a French pressure cell at 12,000 psi. The lysate was then centrifuged at 30,000 × *g* and at 4°C for 45 min, in order to remove cell debris, and Trx was purified as described for MsrP-His_6. Ni-NTA-purified Trx was then loaded on a 120 ml HiLoad 16/60 Superdex 75 PG column (GE healthcare) previously equilibrated with HEPES-KOH 50 mM, pH 7.4, NaCl 100 mM. The resulting Trx-containing fractions were pooled and concentrated using a 5 kDa cutoff Vivaspin 15 device.

Thioredoxin reductase (TrxR) was expressed and purified as follows. BL21 (DE3) cells harboring plasmid pPL223-2, over-expressing TrxR with a N-terminal His_6 tag, were grown aerobically at 37°C in LB supplemented with ampicillin (200 μg/ml). Expression was induced at an A_{600} of 0.6 with 1 mM IPTG during 3 h. Protein extraction was performed as described for Trx and purification was performed as described for MsrP-His_6.

BL21 (DE3) cells harboring plasmid pKD11, over-expressing SurA with a C-terminal His_6 tag, were grown aerobically at 37°C in LB supplemented with kanamycin (50 μg/ml). Expression was induced at an A_{600} of 0.6 with 1 mM IPTG during 3 h. Protein extraction and purification were performed as described for MsrP-His_6.

MG1655 cells harboring plasmid pKD84, over-expressing SurA with a C-terminal *Strep*-tag, were grown aerobically at 37°C in LB supplemented with ampicillin (200 μg/ml). Expression was induced at an A_{600} of 0.7 with a final concentration of 200 μg/l anhydrotetracycline (AHT) during 5 h. Protein extraction was performed as described for MsrP-His_6. SurA-*Strep* was then purified by loading the periplasmic extract on a 5 ml Strep-Tactin Superflow cartridge H-PR (IBA GmbH) equilibrated with buffer A (Tris-HCl 100 mM, pH 8.0, NaCl 150 mM, EDTA 1 mM). After washing the column with buffer A, SurA-*Strep* was eluted by applying a linear gradient of desthiobiotin (from 0 to 2.5 mM) in buffer A. The fractions containing SurA-*Strep* were pooled, concentrated using a 5 kDa cutoff Vivaspin 15 (Sartorius) device and desalted on a PD-10 column (GE Healthcare) equilibrated with 50 mM NaPi, pH 8.0, 150 mM NaCl.

A modified version of Pal lacking the signal sequence and in which the first cysteine of lipobox was replaced by an alanine (Pal_{C1A}) was expressed with an N-terminal His-tag from the pEB0513 vector in BL21 (DE3) cells. Cells were grown aerobically at 37°C in LB

supplemented with ampicillin (200 μg/ml). Expression was induced at an A_{600} of 0.6 with 1 mM IPTG for 3 h. Protein extraction was performed as described for Trx and purification was performed as described for MsrP-His_6.

In vitro repair of oxidized Calmodulin, SurA, and Pal by MsrP

Calmodulin (CaM) was oxidized *in vitro* as described previously [36]. SurA-His_6 and Pal were oxidized *in vitro* by incubating the purified proteins (50 μM) for 2h30 at 30°C with 100 mM H_2O_2 in a buffer containing 50 mM NaPi, pH 8.0, 50 mM NaCl. H_2O_2 was then removed by gel filtration using a NAP-5 column (GE healthcare) equilibrated with 50 mM NaPi, pH 8.0, 150 mM NaCl.

In vitro repair of oxidized CaM (CaMox), SurA (SurA ox) and Pal (Pal ox) was assessed by incubating the oxidized proteins (2 μM of CaMox and SurA ox, 5 μM of Pal ox) with purified MsrP-His_6 (2 μM for CaMox and SurA ox, 5 μM for Pal ox), 10 mM benzyl viologen and an excess of sodium dithionite at 37°C for 1 h. As controls, the oxidized proteins were incubated separately with either MsrP-His_6 or the inorganic reducing system (benzyl viologen and sodium dithionite). The reactions were stopped by adding SB buffer and heating at 95°C for the CaM and SurA samples or by adding 0.1% TFA for the Pal samples. The CaM and SurA samples were then loaded on an SDS-PAGE gel and the proteins visualized with the PageBlue™ Protein Staining Solution (Fermentas). For the Pal samples (20 μg), proteins were separated by reverse-phase HPLC on a C4 column (Vydac 214TP54, 4.6 × 250 mm) at a flow rate of μl400 μl/min with a linear gradient of acetonitrile in 0.1% TFA (0% to 70% acetonitrile in 90 min). Absorbance was monitored at 214 nm and the peaks were collected. The fractions were dried in a Speedvac and the proteins resupsended in 25 μl of 100 mM NH_4HCO_3 prior to overnight digestion at 30°C with 0.5 μg of trypsin or EndoGlu-C. The peptides were then analyzed as described below.

For CaM and SurA, the gel bands corresponding to the different oxidation states were in-gel digested with trypsin and the resulting peptides analyzed by LC-MS/MS on a C18 reverse phase column as described above. Relative abundances of every Met-containing peptide in its different oxidation state were obtained by peak area intensities integration taking into account the extracted ion chromatogram of both doubly and triply charged ions.

In vivo repair of oxidized SurA and Pal by MsrP

The *in vivo* repair of SurA ox and Pal ox by the MsrPQ system or MsrP alone expressed from plasmids pAG195 and pAG192, respectively, was performed as follows. Overnight cultures of AG233 (containing the empty pAG177 vector), AG234 (containing the pAG195 plasmid) and AG289 (containing the pAG192 plasmid) were diluted to an A_{600} of 0.04 into fresh LB medium (100 ml) and cells were grown aerobically at 37°C in the presence of 0.1 mM IPTG and 200 μg/ml ampicillin. At an A_{600} of 0.5, cells were subjected to NaOCl treatment (3.5 mM) and protein synthesis was blocked by the addition of chloramphenicol (300 μg/ml). Samples were taken at different time points after NaOCl addition and precipitated with TCA. The pellets were then washed with ice-cold acetone, suspended in SB buffer, heated at 95°C and loaded on a SDS-PAGE gel for immunoblot analysis using anti-Pal [37] and anti-SurA antibodies. The specificity of the anti-SurA antibody was verified

(Supplementary Figure 6). The protein amounts loaded were standardized by taking into account the A_{600} values of the cultures.

Oxidation, repair and purification of SurA for analysis of chaperone function

SurA-*Strep* was oxidized *in vitro* by incubating the purified protein (200 μM) for 3 h at 30°C with 100 mM H_2O_2 in a buffer containing 50 mM NaPi, pH 8.0, 150 mM NaCl. H_2O_2 was then removed by gel filtration using a NAP-5 column (GE healthcare) equilibrated with 50 mM NaPi, pH 8.0, 150 mM NaCl. For the *in vitro* repair of oxidized SurA (SurA ox), the oxidized protein (30 μM) was incubated with purified MsrP-His_6 (30 μM), 10 mM benzyl viologen and 10 mM of sodium dithionite at 37°C for 1 h. Following repair, SurA was purified by passing the sample through a gravity flow column containing 200 μl Strep-Tactin Sepharose beads (from a 50% suspension, IBA GmbH), previously equilibrated with buffer A (Tris-HCl 100 mM, pH 8.0, NaCl 150 mM, EDTA 1 mM). After washing with buffer A, repaired SurA was eluted using buffer A containing 2.5 mM desthiobiotin. The elution fractions were pooled and submitted to buffer exchange using a NAP-5 column (GE healthcare) equilibrated with 50 mM NaPi, pH 8.0, 150 mM NaCl. To check for the correct oxidation, repair, and purification of SurA, samples were loaded on a SDS-PAGE gel and the proteins visualized with the PageBlue™ Protein Staining Solution (Fermentas).

Analysis of chaperone function

The ability of SurA to act as a chaperone preventing the thermal aggregation of citrate synthase (Sigma, ref. C3260) was assessed as follows. The aggregation of citrate synthase (0.15 μM) was monitored at 43°C in 40 mM HEPES-KOH, pH 7.5 in the absence or in the presence of 0.6 μM SurA, SurA ox or MsrP-repaired SurA ox using light scattering measurements. To avoid effects that may be caused by the protein buffer, all samples were added to the assay in constant volume. SurA ox and MsrP-repaired SurA ox were obtained as described above. Light scattering measurements were made using a Varian Cary Eclipse spectrofluorometer with both excitation and emission wavelengths set to 500 nm at a spectral bandwidth of 2.5 nm. Data points were recorded every 0.1 s.

Genetic analysis of Met-O assimilation

The ability of various *E. coli* strains (BE100, JB08, CH193, BE104) to assimilate Met-O was assessed on M9 minimal medium supplemented with either Met or Met-O at 20 μg/ml. Plates were incubated at 37°C for 72 h. Overnight cultures of strains AG272, AG273, AG279 and AG274 were diluted to an A_{600} of 0.04 into fresh M63 minimal medium (100 ml) supplemented with 0.5% glycerol, 150 μg/ml of each amino acid, 1 mM $MgSO_4$, 1 mM $MoNa_2O_4$, 17 μM $Fe_2(SO_4)_3$, vitamins (thiamin 10 μg/ml, biotin 1 μg/ml, riboflavin 10 μg/ml, and nicotinamide 10 μg/ml) and 100 μg/ml spectinomycin, and grown aerobically at 37°C. When an A_{600} value of 0.5 was reached, cells (5 ml) were washed three times with M63 medium containing 150 μg/ml Met-O instead of methionine, and serially diluted in the same medium. 5 μl of each dilution were then spotted on M63 plates containing either Met or Met-O at 150 μg/ml, and plates were subsequently incubated at 37°C for 40 h.

HOCl induction assays

The *msrP::lacZ* containing strains (CH183, CH186 and CH187) were grown at 37°C with shaking in M9 minimal medium. When cells reached an A_{600} of ~0.2, cultures were split into two plastic tubes, one of them containing HOCl (200 μM), and these tubes were incubated with an inclination of 90° with shaking at 37°C. After 30 minutes of incubation, 1 ml was harvested and the bacteria were resuspended in 1 ml of β-galactosidase buffer. β-galactosidase levels were measured as described [38].

HOCl survival assays

NR744, NR745, CH0127 and AG190 cells were grown aerobically at 37°C with shaking in 50 ml of LB medium in 500 ml flasks. When cells reached an A_{600} of ~0.45, 5 ml samples were transferred to conical polypropylene centrifuge tubes (50 ml; Sarstedt) and HOCl (2 mM) was added. Cells were then incubated at 37°C with shaking (150 rpm) at 90° inclination. Samples were taken at various time points after stress, diluted in PBS buffer, spotted on LB agar and incubated at 37°C for 16 h. Cell survival was determined by counting colony-forming units per ml (c.f.u./ml). The absolute c.f.u at time-point 0 (used as 100%) was ~10^8 cells/ml in all experiments. For strains CH194, CH196 and CH197, the same protocol was used with chloramphenicol (25 μg/ml) and arabinose (0.2%) added to the cultures.

SDS survival assays

Cells (MG1655 and BE107) were grown at 37°C with shaking in 10 ml of LB (in 100 ml flasks). When cells reached an A_{600} of ~0.8, 5 ml samples were transferred to conical polypropylene centrifuge tubes (50 ml, Sarstedt) and HOCl (2 mM) was added. After 5 min of incubation, samples were taken and diluted in PBS buffer to ~2.10^3 cells/ml. 100 μl aliquots were then spread on LB agar plates containing SDS (1%). Colonies were counted the next day.

Dataset construction and phylogenetic analyses

A non-redundant local protein database containing 1,342 complete prokaryotic proteomes available in the NCBI (http://www.ncbi.nlm.nih.gov/) as of July 30, 2014 was built. This database was queried with the BlastP program (default parameters [39], using YedY (NP_416480) and YedZ (NP_416481) of *Escherichia coli* str. K-12 substr. MG1655 as a seed. Distinction between homologous and non-homologous sequences was assessed by visual inspection of each BlastP output (no arbitrary cut-off on the E-value or score). In order to ensure that we did not overlook divergent YedY or YedZ proteins, iterative BlastP queries were performed using homologues identified at each step as new seeds. The list of YedY and YedZ homologs is provided in Supplementary Data 1. The retrieved sequences were aligned using MAFFT version 7 (default parameters [40]. Supplementary Data 2-3). Each alignment was visually inspected and manually refined when necessary using the ED program from the MUST package [41]. Regions where the homology between amino acid positions was doubtful were removed by using BMGE software (BLOSUM30 similarity matrix [42]).

Europe PMC Funders Author Manuscripts

For each homolog, the genomic context was investigated using MGcV (Microbial Genomic context Viewer [43]). The domain composition and protein location of each homolog was also analyzed using pfam version 27.0 [44], SignalP version 4.1 [45] and TMHMM server version 2.0 [46], respectively.

For the YedY protein, preliminary phylogenetic analysis was performed using FastTree v.2 using a gamma distribution with four categories [47]. Based on the resulting tree, the subfamily containing the sequence from *E. coli* was identified and selected for further phylogenetic investigations. The corresponding sequences were realigned using MAFFT version 7. The resulting alignment was trimmed with BMGE as previously described.

Maximum likelihood (ML) trees were computed using PHYML version 3.1 [48] with the Le and Gascuel (LG) model (amino acid frequencies estimated from the dataset) and a gamma distribution (4 discrete categories of sites and an estimated alpha parameter) to take into account evolutionary rate variations across sites. Branch robustness was estimated by the non-parametric bootstrap procedure implemented in PhyML (100 replicates of the original dataset with the same parameters). Bayesian inferences (BI) were performed using MrBayes 3.2 [49] with a mixed model of amino acid substitution including a gamma distribution (4 discrete categories). MrBayes was run with four chains for 1 million generations and trees were sampled every 100 generations. To construct the consensus tree, the first 2000 trees were discarded as “burn in”.

Europe PMC Funders Author Manuscripts

Extended Data

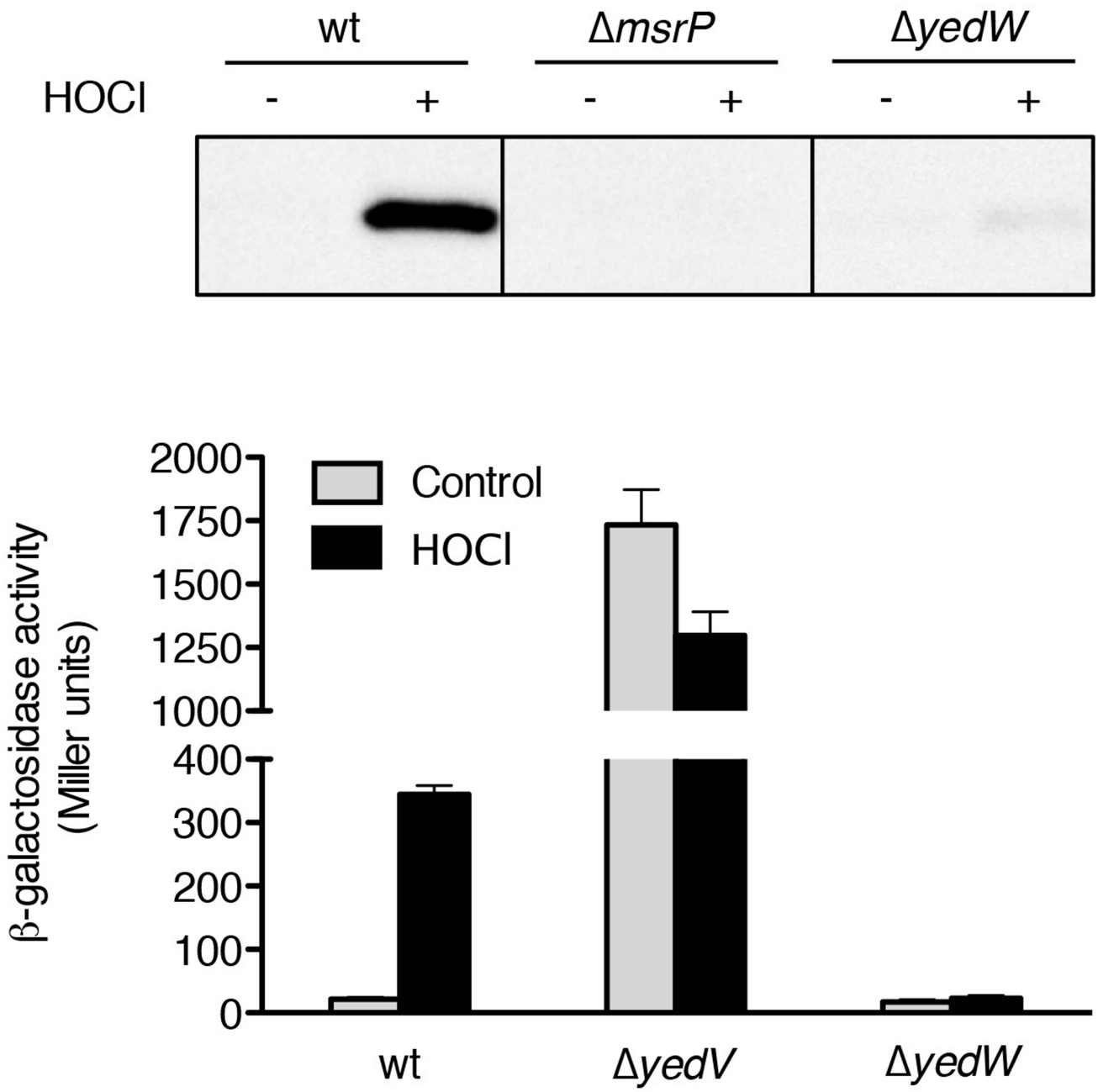

Extended Data Figure 1. Induction of MsrPQ by HOCl is dependent on the presence of a functional YedVW two-component system

Upper panel: immunoblot analysis shows that the induction of MsrP synthesis by HOCl (0.2 mM) is *yedW*-dependent. The image is representative of experiments made in biological triplicate. Lower panel: an *msrP::lacZ* fusion was used as a read-out for *msrP* expression. Deletion of *yedV* upregulates *msrP* expression, while deletion of *yedW* prevents its induction by HOCl. Error bars represent mean ± s.e.m.; n=4. The uncropped blot is shown in Supplementary Figure 4.

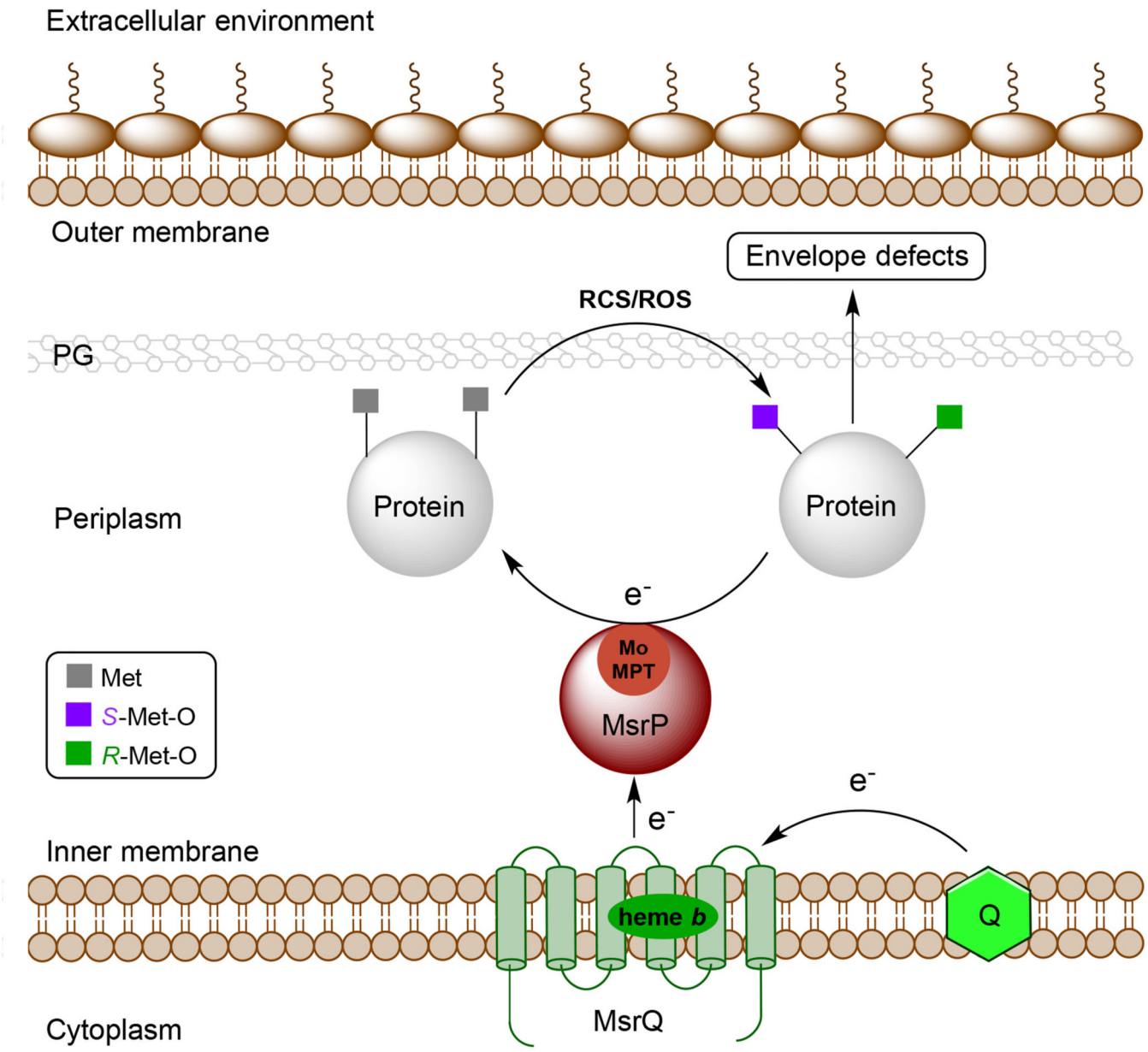

Extended Data Figure 2. Respiratory chain-powered, non-stereospecific reduction of Met-O in periplasmic proteins by the MsrPQ system maintains envelope integrity

Upon exposure to RCS and/or ROS, methionine residues (Met) in periplasmic proteins such as SurA and Pal get oxidized and randomly form either the *R* or the *S* diastereoisomer of methionine sulfoxide (Met-O). This results in the loss of function of some proteins important for maintaining the integrity of the envelope, such as SurA, giving rise to envelope defects. MsrP catalyzes the reduction of both diastereoisomers of Met-O with the help of its molybdenum-molybdopterin (Mo-MPT) cofactor. Electrons for reduction are provided by the quinone (Q) pool of the respiratory chain through MsrQ, the IM heme *b*-containing partner of MsrP. PG= peptidoglycan.

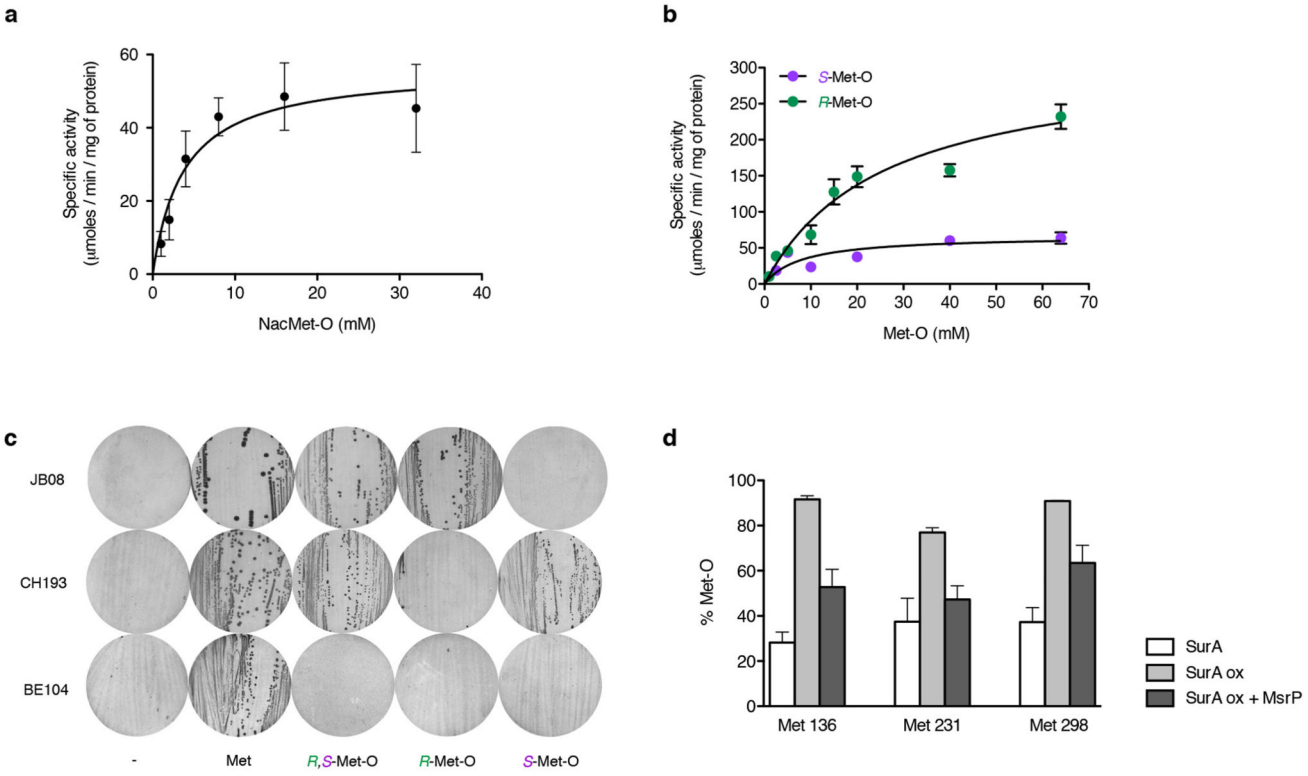

Extended Data Figure 3. MsrP non-stereospecifically reduces Met-O

a. MsrP reduces N-acetyl-Met-O (NacMet-O), a substrate mimicking protein-bound Met-O, with a K_m of 3.8 ± 1.2 mM, a k_{cat} of 30.5 ± 3.1 s^{-1} and a V_{max} of 56.3 ± 5.8 µmoles/min/mg protein (error bars represent mean ± s.d.; *n*=3). **b.** MsrP is a non-stereospecific Msr, being able to reduce both *S*-Met-O (with a K_m of 8.0 ± 2.7 mM, a k_{cat} of 36.0 ± 3.6 s^{-1} and a V_{max} of 67.2 ± 6.4 µmoles/min/mg protein) and *R*-Met-O **(**with a K_m of 25.7 ± 4.7 mM, a k_{cat} of 168.3 ± 15.0 s^{-1} and a V_{max} of 313.4 ± 27.6 µmoles/min/mg protein). Error bars represent mean ± s.d.; *n*=3. **c.** Strain JB08 (Met^- $MsrA^-$ $MsrB^-$ $BisC^-$, producing MsrC) is able to grow only on *R*-Met-O, whereas strain CH193 (Met^- $MsrA^-$ $MsrB^-$ $MsrC^-$, producing BisC) in only able to grow on *S*-Met-O. Deletion of *msrP* in strain BE100 (Met^- Msr^- $Sup^{Met\text{-}O^+}$) prevents its growth on *R*- and *S*-Met-O (strain BE104 = Met^- Msr^- $Sup^{Met\text{-}O^+}$ Δ*msrP*, compare to growth of BE100 in Fig. 2e). Images are representative of experiments made in biological triplicate. **d.** The periplasmic chaperone SurA was treated with H_2O_2, giving rise to SurA ox, a sample of which was subsequently incubated with MsrP and the inorganic reducing system *in vitro*. The oxidation state of specific Met residues (Met 136, 231, and 298) in the various samples was determined by LC-MS/MS analysis. Error bars represent mean ± s.e.m.; *n*=4.

Europe PMC Funders Author Manuscripts

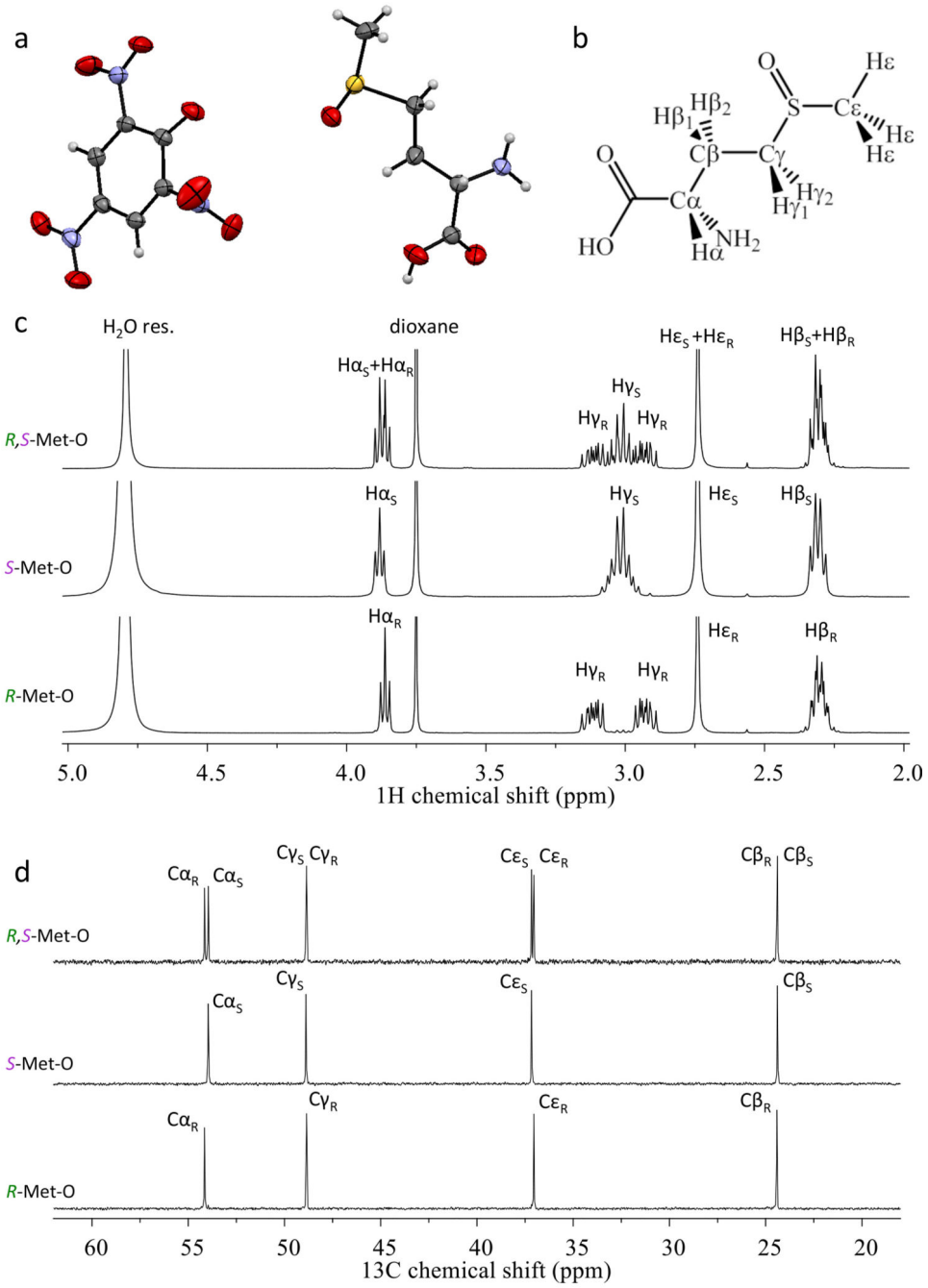

Extended Data Figure 4. Preparation of pure diastereoisomeric forms of Met-O

a. The Oak Ridge Thermal Ellipsoid Plot (ORTEP ellipsoid) representation with 50% probability level of the crystal structure for the isolated salt of L-methionine-*S*-sulfoxide (right) picrate (left). The grey, blue, red, white and yellow spheres respectively represent carbon, nitrogen, oxygen, hydrogen, and sulfur atoms. **b.** Chemdraw representation of L-methionine-*R, S*-sulfoxide with proton and carbon positioning (relative to NMR assignment). **c.** Zoom on the ^{1}H NMR spectra of ~ 150 mM solutions of L-methionine sulfoxide in D_2O pD 6.5, either as a mixture of *R*- and *S*- diastereoisomers (top), isolated *S*-

(middle), or isolated *R*- (bottom) (containing 30 mM dioxane as an internal reference). **d.** Zoom on the ^{13}C NMR spectra of ~ 150 mM solutions of L-methionine sulfoxide in D_2O pD 6.5, either as a mixture of *R*- and *S*- diastereoisomers (top), isolated *S*- (middle), or isolated *R*- (bottom) (containing 30 mM dioxane as an internal reference).

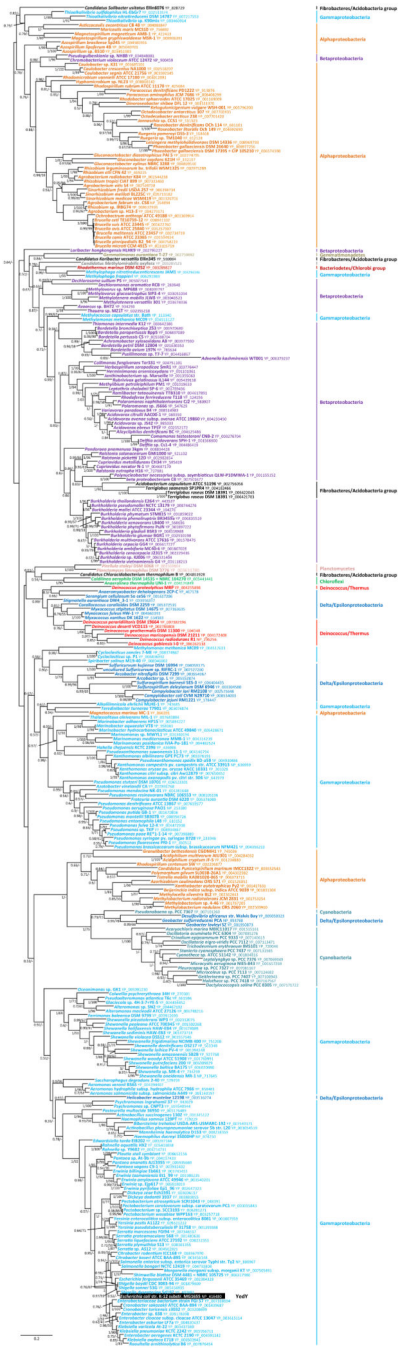

Extended Data Figure 5. Individual phylogenies of YedY

Shown are unrooted Bayesian phylogenetic trees for YedY (b1971, 310 sequences, 260 positions). Numbers at nodes indicate posterior probabilities (PP) computed by MrBayes [49]

Europe PMC Funders Author Manuscripts

Europe PMC Funders Author Manuscripts

and bootstrap values (BV) computed by PhyML [48]. Only PP and BV above 0.5 and 50%, respectively, are shown. The scale bars represent the average number of substitutions per site. In the phylogenetic tree, YedY from *E. coli* is highlighted in grey.

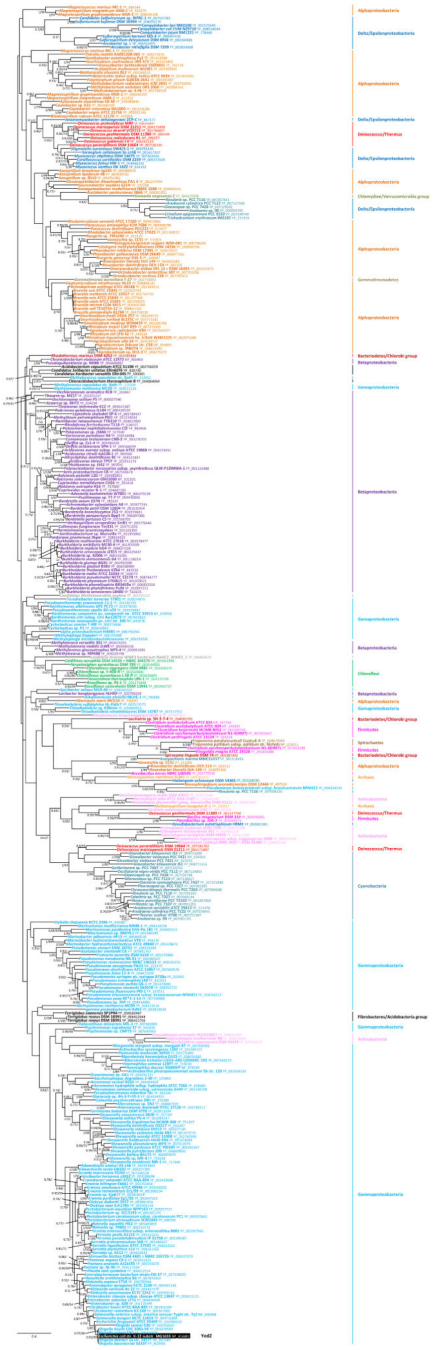

Extended Data Figure 6. Individual phylogenies of YedZ

Shown are unrooted Bayesian phylogenetic trees for YedZ (b1972, 369 sequences, 135 positions). Numbers at nodes indicate posterior probabilities (PP) computed by MrBayes [49] and bootstrap values (BV) computed by PhyML [48]. Only PP and BV above 0.5 and 50%,

respectively, are shown. The scale bars represent the average number of substitutions per site. In the phylogenetic tree, YedZ from *E. coli* is highlighted in grey.

Extended Data Table 1.
The MsrPQ system uses electrons from respiratory chain to reduce free Met-O

This table shows the ability of the various strains to grow (+) or not (−) using Met-O as sole Met source. Strains were grown for 40 to 72h at 37°C. The results are representative of experiments made in biological triplicate.

Strain description	Met	Met-O
Met$^-$	+	+
Met$^-$ Msr$^-$ (JB590)	+	−
Met$^-$ Msr$^-$ Sup$^{Met\text{-}O+}$ (BE100)	+	+
Met$^-$ Msr$^-$ Sup$^{Met\text{-}O+}$ Δ*yedZ*(BE105)	+	−
Met$^-$ Msr$^-$ empty vector (AG272)	+	−
Met$^-$ Msr$^-$ p*yedY* (AG273)	+	−
Met$^-$ Msr$^-$ p*yedZ* (AG279)	+	−
Met$^-$ Msr$^-$ p*yedYyedZ* (AG274)	+	+
Met$^-$ Msr$^-$ Sup$^{Met\text{-}O+}$ Δ*menA* Δ*ubiE* (BE106)	+	−

Extended Data Table 2.
List of proteins identified as potential MsrP substrates

Semi-quantitative 2D-LC-MS/MS analysis was used to identify proteins that have one or more oxidized Met residues that MsrP could reduce. The first column indicates the name of the protein, the second describes its function and the third gives the number and % of methionine residues in the mature protein (excluding the signal sequence).

Protein	Function	Number and percentage of methionines in the protein*
SurA	Primary periplasmic chaperone	14 (3.4%)
LolA	Outer-membrane lipoprotein carrier protein	2 (1.1%)
Pal	Peptidoglycan-associated lipoprotein	6 (3.9%)
MlaC	Probable phospholipid-binding protein	4 (2.1%)
PpiA	Peptidyl-prolyl cis-trans isomerase A	4 (2.4%)
DsbA	Thiol:disulfide interchange protein	6 (3.2%)
CysP	Thiosulfate-binding protein	4 (1.3%)
PotD	Spermidine/putrescine-binding periplasmic protein	9 (2.8%)
MppA	Periplasmic murein peptide-binding protein	7 (1.4%)
ProX	Glycine betaine-binding periplasmic protein	6 (1.9%)
MalE	Maltose-binding periplasmic protein	6 (1.6%)
MglB	D-galactose-binding periplasmic protein	6 (1.9%)
RbsB	D-ribose-binding periplasmic protein	4 (1.5%)
FecB	Fe^{3+} dicitrate-binding periplasmic protein	7 (2.5%)

Protein	Function	Number and percentage of methionines in the protein*
RcnB	Nickel/cobalt homeostasis protein	2 (2.3%)
ZnuA	High-affinity zinc uptake system protein	6 (2.1%)
Ecotin	General inhibitor of pancreatic serine proteases	4 (2.8%)
Ivy	Inhibitor of vertebrate lysozyme	5 (3.9%)
PspE	Thiosulfate sulfurtransferase	2 (2.4%)
YmgD	Uncharacterized protein	4 (4.4%)

*Referring to the mature protein without its signal sequence

Supplementary Material

Refer to Web version on PubMed Central for supplementary material.

ACKNOWLEDGEMENTS

We thank Asma Boujtat, Gaëtan Herinckx and Jean-Pierre Szikora for technical and computational help and the members of the Barras and Collet laboratories for discussions. We are indebted to Monique Sabbaty and David Pignol for sharing unpublished information, to Tom Silhavy, Tracy Palmer, Emmanuelle Bouveret and Diarmaid Hughes for providing strains and plasmids, to Todd Lowther and Marius Réglier for advice and discussions and to Nassos Typas, Tâm Mignot, Joris Messens, Jim Bardwell and Francis-André Wollman for reading the manuscript and providing comments. A.G. and J.S. are research fellows of the FRIA, P.L. is “Chargée de Recherche” and J.-F.C. is “Maître de Recherche” of the FRS-FNRS. E.O. is supported by a grant from Indo French Center for the Promotion of the Advanced Research CEFIPRA “(5105-2)”. R.A. is supported by the Fonds Maurange, Fondation Roi Baudouin. This work was supported, in part, by grants from the FRS-FNRS and from the European Research Council (FP7/2007–2013) ERC independent researcher starting grant 282335 – Sulfenic to J.-F.C. and funding by CNRS, FRM and Aix-Marseille Université to the F.B. team.

REFERENCES

1. Boschi-Muller S, Gand A, Branlant G. The methionine sulfoxide reductases: Catalysis and substrate specificities. Archives of biochemistry and biophysics. 2008; 474:266–273. doi:10.1016/j.abb.2008.02.007. [PubMed: 18302927]
2. Ezraty B, Aussel L, Barras F. Methionine sulfoxide reductases in prokaryotes. Biochim Biophys Acta. 2005; 1703:221–229. doi:10.1016/j.bbapap.2004.08.017. [PubMed: 15680230]
3. Lee BC, Gladyshev VN. The biological significance of methionine sulfoxide stereochemistry. Free radical biology & medicine. 2011; 50:221–227. doi:10.1016/j.freeradbiomed.2010.11.008. [PubMed: 21075204]
4. Urano H, Umezawa Y, Yamamoto K, Ishihama A, Ogasawara H. Cooperative regulation of the common target genes between hydrogen peroxide-response YedVW and copper-response CusSR in Escherichia coli. Microbiology. 2015 doi:10.1099/mic.0.000026.
5. Loschi L, et al. Structural and biochemical identification of a novel bacterial oxidoreductase. J Biol Chem. 2004; 279:50391–50400. doi:10.1074/jbc.M408876200. [PubMed: 15355966]
6. Workun GJ, Moquin K, Rothery RA, Weiner JH. Evolutionary persistence of the molybdopyranopterin-containing sulfite oxidase protein fold. Microbiol Mol Biol Rev. 2008; 72:228–248. table of contents, doi:10.1128/MMBR.00041-07. [PubMed: 18535145]
7. Melnyk RA, et al. Novel mechanism for scavenging of hypochlorite involving a periplasmic methionine-rich Peptide and methionine sulfoxide reductase. mBio. 2015; 6:e00233–00215. doi:10.1128/mBio.00233-15. [PubMed: 25968643]
8. Stewart EJ, Aslund F, Beckwith J. Disulfide bond formation in the Escherichia coli cytoplasm: an in vivo role reversal for the thioredoxins. Embo J. 1998; 17:5543–5550. [PubMed: 9755155]

9. Brokx SJ, Rothery RA, Zhang G, Ng DP, Weiner JH. Characterization of an Escherichia coli sulfite oxidase homologue reveals the role of a conserved active site cysteine in assembly and function. Biochemistry. 2005; 44:10339–10348. doi:10.1021/bi050621a. [PubMed: 16042411]
10. Tarrago L, Gladyshev VN. Recharging oxidative protein repair: catalysis by methionine sulfoxide reductases towards their amino acid, protein, and model substrates. Biochemistry. Biokhimiia. 2012; 77:1097–1107. doi:10.1134/S0006297912100021. [PubMed: 23157290]
11. Lowe RH, Evans HJ. Preparation and Some Properties of a Soluble Nitrate Reductase from Rhizobium Japonicum. Biochim Biophys Acta. 1964; 85:377–389. [PubMed: 14194853]
12. Le DT, et al. Analysis of methionine/selenomethionine oxidation and methionine sulfoxide reductase function using methionine-rich proteins and antibodies against their oxidized forms. Biochemistry. 2008; 47:6685–6694. doi:10.1021/bi800422s. [PubMed: 18505275]
13. Silhavy TJ, Kahne D, Walker S. The bacterial cell envelope. Cold Spring Harbor perspectives in biology. 2010; 2:a000414. doi:10.1101/cshperspect.a000414. [PubMed: 20452953]
14. Goemans C, Denoncin K, Collet JF. Folding mechanisms of periplasmic proteins. Biochim Biophys Acta. 2014; 1843:1517–1528. doi:10.1016/j.bbamcr.2013.10.014. [PubMed: 24239929]
15. Sklar JG, Wu T, Kahne D, Silhavy TJ. Defining the roles of the periplasmic chaperones SurA, Skp, and DegP in Escherichia coli. Genes Dev. 2007; 21:2473–2484. doi:21/19/2473 [pii] 10.1101/gad.1581007. [PubMed: 17908933]
16. Denoncin K, Schwalm J, Vertommen D, Silhavy TJ, Collet JF. Dissecting the Escherichia coli periplasmic chaperone network using differential proteomics. Proteomics. 2012; 12:1391–1401. doi:10.1002/pmic.201100633. [PubMed: 22589188]
17. Ruiz N, Falcone B, Kahne D, Silhavy TJ. Chemical conditionality: a genetic strategy to probe organelle assembly. Cell. 2005; 121:307–317. [PubMed: 15851036]
18. Brot N, et al. The thioredoxin domain of Neisseria gonorrhoeae PilB can use electrons from DsbD to reduce downstream methionine sulfoxide reductases. J Biol Chem. 2006; 281:32668–32675. [PubMed: 16926157]
19. Cho SH, Collet JF. Many roles of the bacterial envelope reducing pathways. Antioxid Redox Signal. 2013; 18:1690–1698. doi:10.1089/ars.2012.4962. [PubMed: 23025488]
20. Hitchcock A, et al. Roles of the twin-arginine translocase and associated chaperones in the biogenesis of the electron transport chains of the human pathogen Campylobacter jejuni. Microbiology. 2010; 156:2994–3010. doi:10.1099/mic.0.042788-0. [PubMed: 20688826]
21. Spector D, Etienne F, Brot N, Weissbach H. New membrane-associated and soluble peptide methionine sulfoxide reductases in Escherichia coli. Biochem Biophys Res Commun. 2003; 302:284–289. [PubMed: 12604343]
22. Baba T, et al. Construction of Escherichia coli K-12 in-frame, single-gene knockout mutants: the Keio collection. Mol Syst Biol. 2006; 2:2006–0008. doi:msb4100050 [pii] 10.1038/msb4100050. [PubMed: 16738554]
23. Bremer E, Silhavy TJ, Weisemann JM, Weinstock GM. Lambda placMu: a transposable derivative of bacteriophage lambda for creating lacZ protein fusions in a single step. J Bacteriol. 1984; 158:1084–1093. [PubMed: 6327627]
24. Datsenko KA, Wanner BL. One-step inactivation of chromosomal genes in Escherichia coli K-12 using PCR products. Proc Natl Acad Sci U S A. 2000; 97:6640–6645. doi:10.1073/pnas.120163297 120163297 [pii]. [PubMed: 10829079]
25. Mandin P, Gottesman S. A genetic approach for finding small RNAs regulators of genes of interest identifies RybC as regulating the DpiA/DpiB two-component system. Mol Microbiol. 2009; 72:551–565. doi:10.1111/j.1365-2958.2009.06665.x. [PubMed: 19426207]
26. Gottlieb HE, Kotlyar V, Nudelman A. NMR Chemical Shifts of Common Laboratory Solvents as Trace Impurities. The Journal of organic chemistry. 1997; 62:7512–7515. [PubMed: 11671879]
27. Holland HL. Tetrahedron-Assymetr. 1999; 10:2833.
28. Lavine TF. The formation, resolution, and optical properties of the diastereoisomeric sulfoxides derived from L-methionine. J Biol Chem. 1947; 169:477–491. [PubMed: 20259080]
29. Koc A, Gasch AP, Rutherford JC, Kim HY, Gladyshev VN. Methionine sulfoxide reductase regulation of yeast lifespan reveals reactive oxygen species-dependent and -independent

Europe PMC Funders Author Manuscripts

components of aging. Proc Natl Acad Sci U S A. 2004; 101:7999–8004. doi:10.1073/pnas.0307929101. [PubMed: 15141092]

30. Lherbet C, Gravel C, Keillor JW. Synthesis of S-alkyl L-homocysteine analogues of glutathione and their kinetic studies with gamma-glutamyl transpeptidase. Bioorganic & medicinal chemistry letters. 2004; 14:3451–3455. doi:10.1016/j.bmcl.2004.04.072. [PubMed: 15177451]
31. Vertommen D, et al. The disulphide isomerase DsbC cooperates with the oxidase DsbA in a DsbD-independent manner. Mol Microbiol. 2008; 67:336–349. doi:10.1111/j.1365-2958.2007.06030.x. [PubMed: 18036138]
32. Arts IS, et al. Dissecting the machinery that introduces disulfide bonds in Pseudomonas aeruginosa. mBio. 2013; 4:e00912–00913. doi:10.1128/mBio.00912-13. [PubMed: 24327342]
33. Vizcaíno JA, et al. ProteomeXchange provides globally co-ordinated proteomics data submission and dissemination. Nature Biotechnol. 2004; 30:223–226. [PubMed: 24727771]
34. Roberts DM, et al. Chemical synthesis and expression of a calmodulin gene designed for site-specific mutagenesis. Biochemistry. 1985; 24:5090–5098. [PubMed: 3000422]
35. Grimaud R, et al. Repair of oxidized proteins. Identification of a new methionine sulfoxide reductase. J Biol Chem. 2001; 276:48915–48920. doi:10.1074/jbc.M105509200. [PubMed: 11677230]
36. Tsvetkov PO, et al. Calorimetry and mass spectrometry study of oxidized calmodulin interaction with target and differential repair by methionine sulfoxide reductases. Biochimie. 2005; 87:473–480. doi:10.1016/j.biochi.2004.11.020. [PubMed: 15820754]
37. Cascales E, Bernadac A, Gavioli M, Lazzaroni JC, Lloubes R. Pal lipoprotein of *Escherichia coli* plays a major role in outer membrane integrity. J Bacteriol. 2002; 184:754–759. [PubMed: 11790745]
38. Miller, J. A Short Course in Bacterial Genetics. Cold Spring Harbor Lab. Press; Plainview, NY: 1992.
39. Altschul SF, et al. Gapped BLAST and PSI-BLAST: a new generation of protein database search programs. Nucleic Acids Res. 1997; 25:3389–3402. [PubMed: 9254694]
40. Katoh K, Standley DM. MAFFT multiple sequence alignment software version 7: improvements in performance and usability. Molecular biology and evolution. 2013; 30:772–780. doi:10.1093/molbev/mst010. [PubMed: 23329690]
41. Philippe H. MUST, a computer package of Management Utilities for Sequences and Trees. Nucleic Acids Res. 1993; 21:5264–5272. [PubMed: 8255784]
42. Criscuolo A, Gribaldo S. BMGE (Block Mapping and Gathering with Entropy): a new software for selection of phylogenetic informative regions from multiple sequence alignments. BMC evolutionary biology. 2010; 10:210. doi:10.1186/1471-2148-10-210. [PubMed: 20626897]
43. Overmars L, Kerkhoven R, Siezen RJ, Francke C. MGcV: the microbial genomic context viewer for comparative genome analysis. BMC genomics. 2013; 14:209. doi:10.1186/1471-2164-14-209. [PubMed: 23547764]
44. Finn RD, et al. Pfam: the protein families database. Nucleic Acids Res. 2014; 42:D222–230. doi:10.1093/nar/gkt1223. [PubMed: 24288371]
45. Petersen TN, Brunak S, von Heijne G, Nielsen H. SignalP 4.0: discriminating signal peptides from transmembrane regions. Nature methods. 2011; 8:785–786. doi:10.1038/nmeth.1701. [PubMed: 21959131]
46. Sonnhammer EL, von Heijne G, Krogh A. A hidden Markov model for predicting transmembrane helices in protein sequences. Proceedings / … International Conference on Intelligent Systems for Molecular Biology ; ISMB. International Conference on Intelligent Systems for Molecular Biology. 1998; 6:175–182. [PubMed: 9783223]
47. Price MN, Dehal PS, Arkin AP. FastTree 2--approximately maximum-likelihood trees for large alignments. PloS one. 2010; 5:e9490. doi:10.1371/journal.pone.0009490. [PubMed: 20224823]
48. Guindon S, et al. New algorithms and methods to estimate maximum-likelihood phylogenies: assessing the performance of PhyML 3.0. Systematic biology. 2010; 59:307–321. doi:10.1093/sysbio/syq010. [PubMed: 20525638]

49. Ronquist F, et al. MrBayes 3.2: efficient Bayesian phylogenetic inference and model choice across a large model space. Systematic biology. 2012; 61:539–542. doi:10.1093/sysbio/sys029. [PubMed: 22357727]

Europe PMC Funders Author Manuscripts

Europe PMC Funders Author Manuscripts

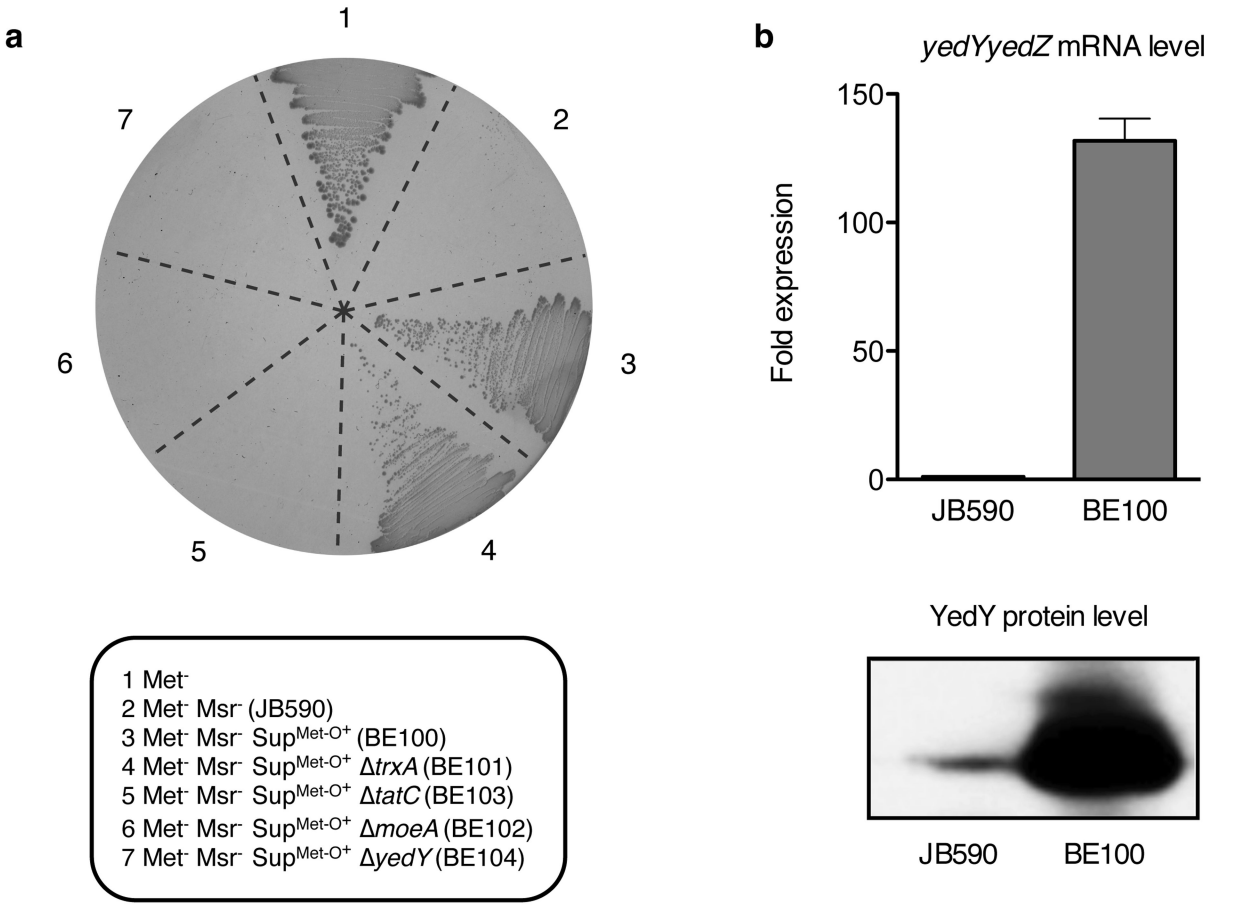

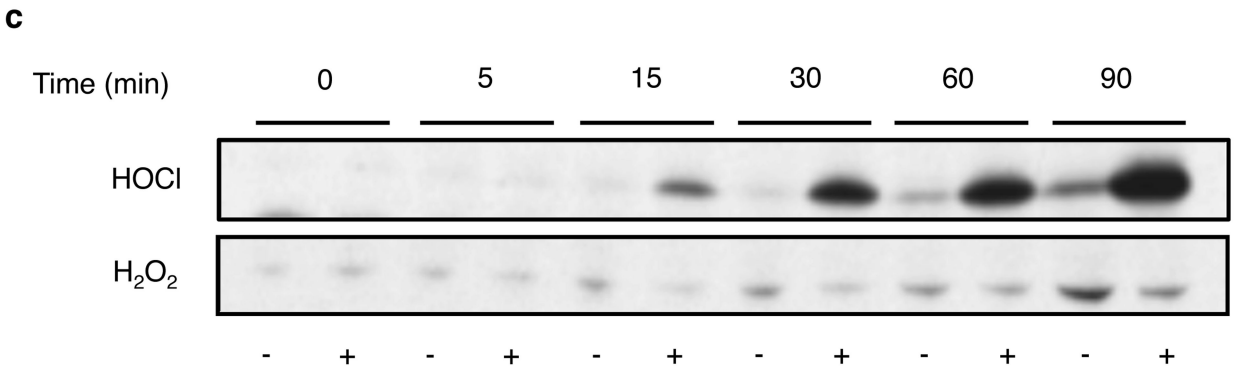

Figure 1. The MsrPQ system reduces free Met-O and is induced by HOCl

a. JB590, a methionine auxotroph (Met$^-$, #1), lacking all cytoplasmic Msrs (Met$^-$ Msr$^-$, #2), cannot grow on Met-O as the only Met source in contrast to suppressor BE100 (Met$^-$ Msr$^-$ Sup$^{Met\text{-}O+}$, #3). Deletion of *yedY* (renamed *msrP*, #7), *moeA* (#6) and *tatC* (#5), but not of *trxA* (#4), prevents the growth of BE100. **b.** The *yedYZ* operon is upregulated in BE100. The increase is observed both at the mRNA (RT-qPCR, upper panel; error bars represent mean ± s.e.m.; n=3) and protein (western blot, lower panel) levels. The RT-qPCR primers were designed to quantify the *yedY-yedZ* mRNA. **c.** Immunoblot analysis showing that

HOCl (2 mM), but not H_2O_2 (1 mM), induces YedY synthesis in a wild-type strain. The images in parts **a, b** and **c** are representative of experiments made in biological triplicate. Uncropped blots are in Supplementary Figure 1.

Europe PMC Funders Author Manuscripts

Europe PMC Funders Author Manuscripts

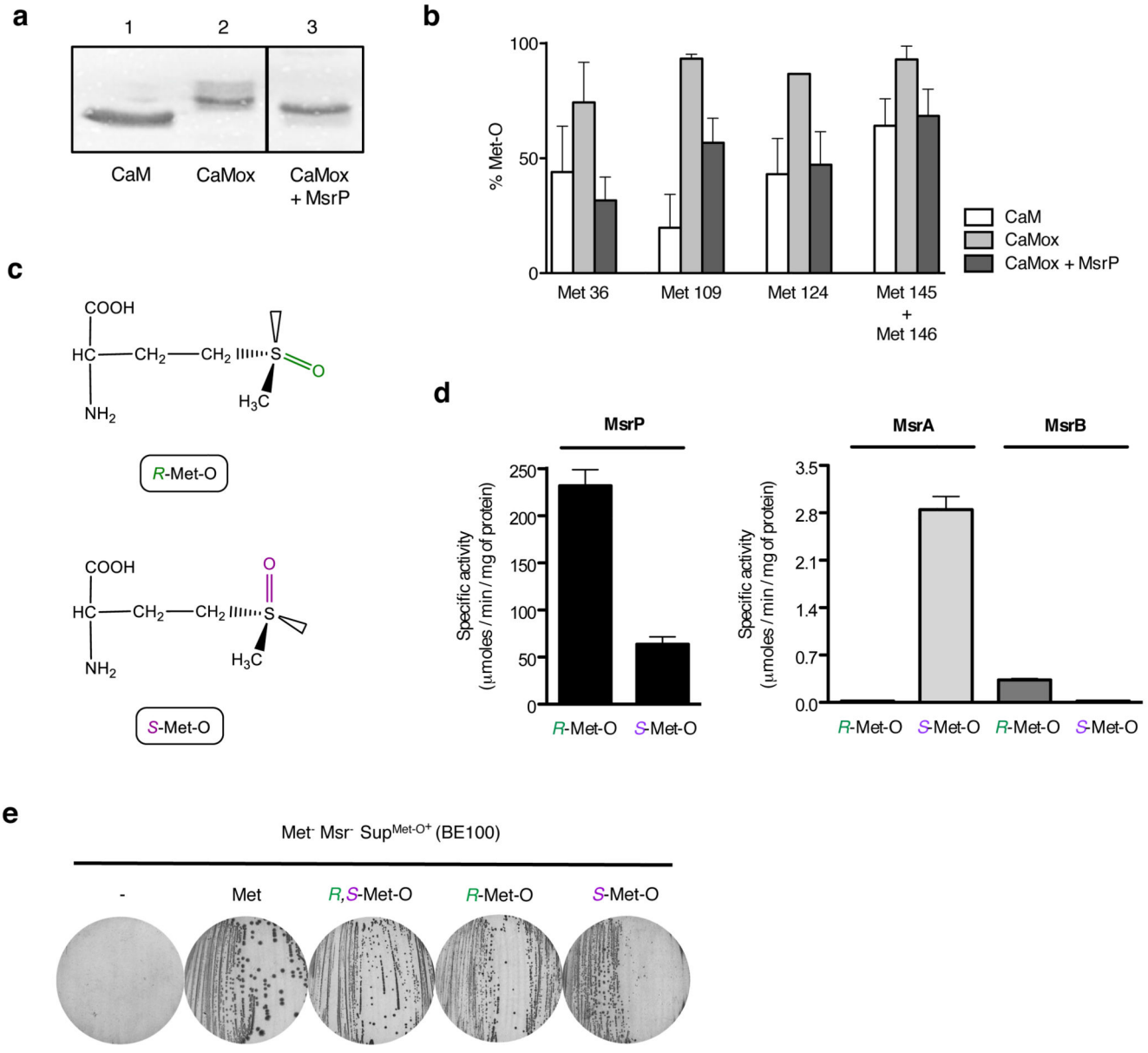

Figure 2. MsrP non-stereospecifically reduces protein-bound Met-O

a. Oxidation of Met in calmodulin (CaM) by H_2O_2 leads to a mobility shift of the oxidized protein (CaMox); compare lane 2 to lane 1. Incubation of CaMox with MsrP and a reducing system involving dithionite and benzyl viologen restores the mobility (lane 3). **b.** MsrP can reduce Met-O in CaMox. The oxidation state of peptides containing either Met36, Met109, Met124 or Met145-146 was determined by LC-MS/MS. Error bars represent mean ± s.e.m.; n=4 for Met36, 109 and 145-146; n=5 for Met124. Met-O residues were detected in the untreated and MsrP-treated samples due to limitations inherent to the methodology applied and oxidation of the samples during analytical handling. **c.** Schematic representation of the two diastereoisomers of Met-O, *R*-Met-O and *S*-Met-O. **d.** MsrP exhibits activity towards both diastereoisomers (left panel), contrary to the stereospecific enzymes MsrA and MsrB (right panel). Specific activities were assayed using 64 mM of either *R*- or *S*-Met-O. Error

bars represent mean ± s.d.; n=3. **e.** The suppressor BE100 is able to grow on both isoforms of Met-O. The images in parts **a** and **e** are representative of experiments made in biological triplicate. The uncropped gel is in Supplementary Figure 2.

Europe PMC Funders Author Manuscripts

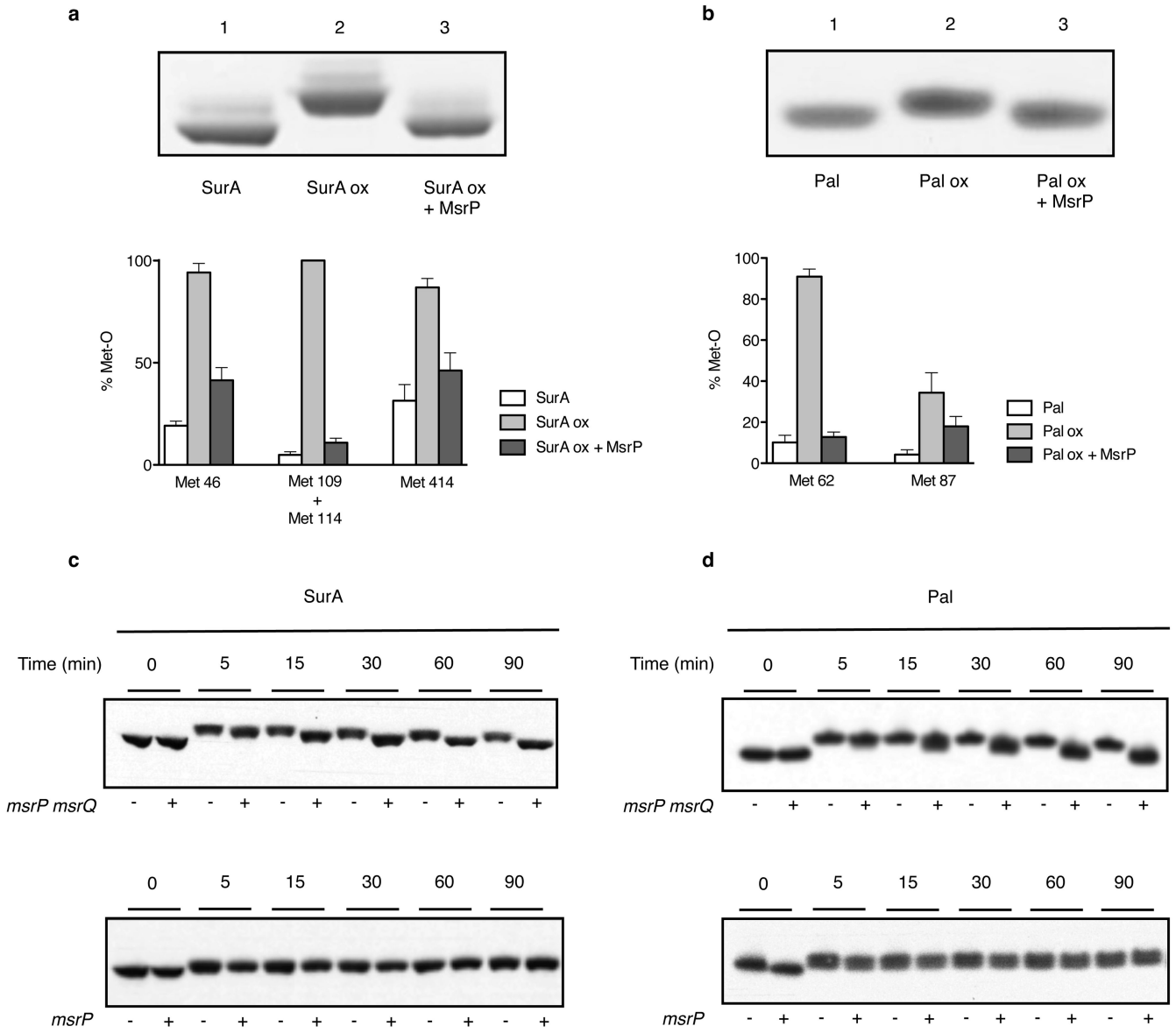

Figure 3. The MsrPQ system rescues oxidized Met residues in SurA and Pal

a, b. Oxidation of SurA (SurA ox) and Pal (Pal ox) by H_2O_2 leads to a mobility shift resulting from Met-O formation. Incubation with MsrP and the inorganic reducing system restores their mobility (upper panels). The percentages of Met-O in the various samples were determined by LC-MS/MS analysis, confirming that MsrP reduces Met-O in SurA and Pal (lower panels). Error bars represent mean ± s.e.m.; n=3. Met-O residues were detected in the untreated and MsrP-treated samples due to limitations inherent to the methodology applied and oxidation of the samples during analytical handling. **c, d.** Δ*msrPQ* cells carrying *msrP* either alone or with *msrQ* under an IPTG-inducible promoter on a plasmid (pAG192 and pAG195, respectively) were grown with IPTG (100 μM). Cells were treated with chloramphenicol (300 μg/ml) at an OD_{600} of 0.5 to block new protein synthesis and HOCl (3.5 mM) was added. Synthesis of MsrP and MsrQ together (upper panels), but not of MsrP

Europe PMC Funders Author Manuscripts

alone (lower panels), restores SurA and Pal mobility. The images in **a, b, c** and **d** are representative of experiments made in biological triplicate. The small shift exhibited by SurA over-time in the absence of MsrPQ could be due to a residual Msr activity, possibly a NADPH-dependent membrane-bound Msr activity detected by Spector *et al.* [21]. Uncropped gels and blots are in Supplementary Figure 3.

Europe PMC Funders Author Manuscripts

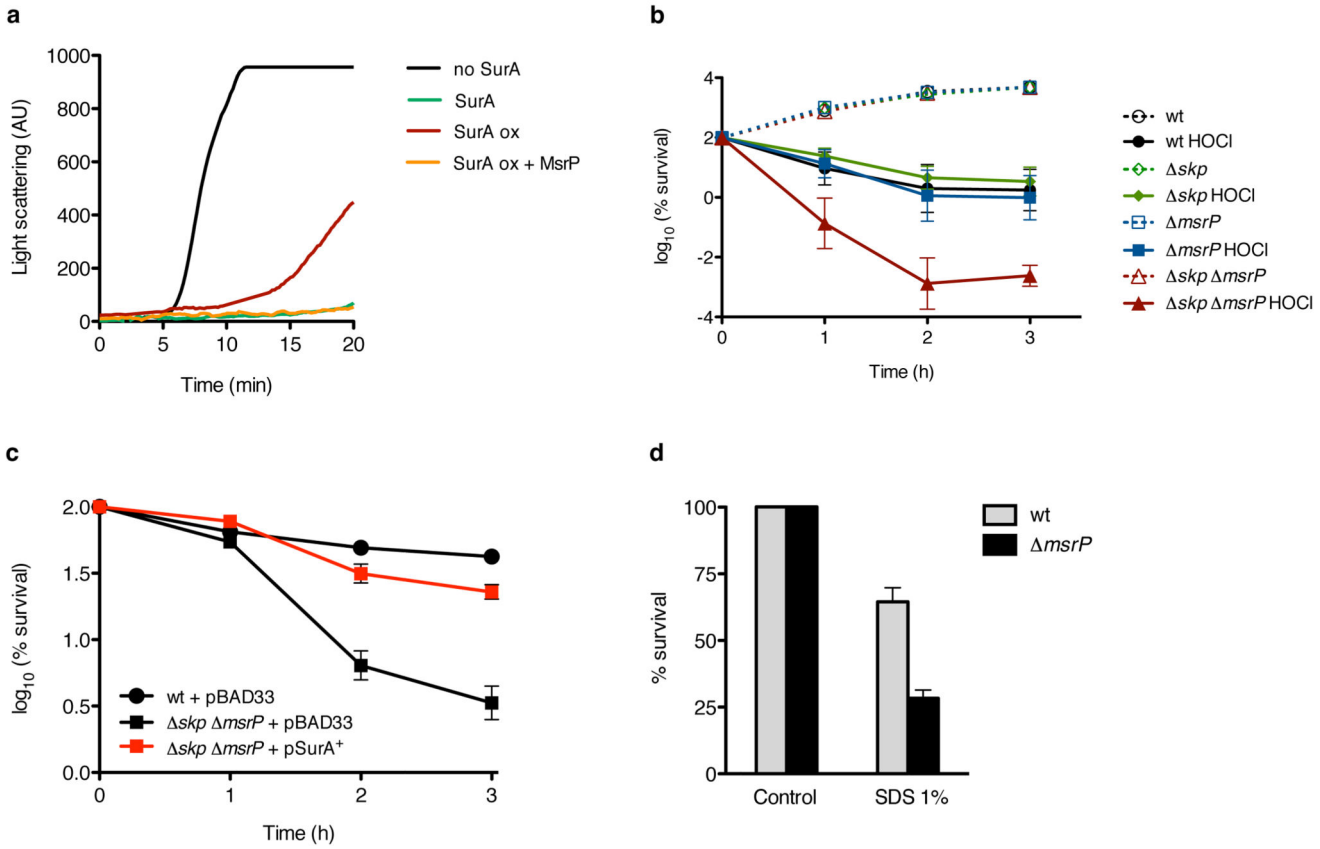

Figure 4. The reducing activity of the MsrPQ system is important for envelope integrity

a. Repair of oxidized SurA (SurA ox) by MsrP (SurA ox + MsrP) restores the ability of SurA to protect thermally-unfolded citrate synthase from aggregation. The graph is representative of experiments made in biological triplicate (AU, arbitrary units). **b.** While the wild type (wt), the Δ*skp* and the Δ*msrP* strains are only moderately affected by exposure to HOCl (2 mM), the viability of the Δ*skp* Δ*msrP* mutant (in which SurA is essential) is decreased. Error bars represent mean ± s.e.m.; n=3. **c.** The sensitivity of the Δ*skp* Δ*msrP* mutant to HOCl is suppressed by SurA overexpression. Error bars represent mean ± s.e.m.; n=4. **d.** Pre-treatment with HOCl renders the Δ*msrP* mutant hypersensitive to SDS, indicative of envelope defects. Error bars represent mean ± s.e.m.; n=3.

Europe PMC Funders Author Manuscripts